STUDY OF COMPETING CHARGE, SPIN AND SUPERCONDUCTING ORDERS IN UNDERDOPED HIGH-TEMPERATURE SUPERCONDUCTORS.

By

Urga Dinegde

A Dissertation submitted to the

department of physics

of Addis Ababa University

in partial fulfillment of the requirements for the Degree of

Doctor of Philosophy in Physics

Addis Ababa

Ethiopia

March 2018

ADDIS ABABA UNIVERSITY

SCHOOL OF GRADUATE STUDIES

This is to certify that the dissertation prepared by Urga Dinegde Yadete, entitled " study of competing charge, spin and superconducting orders in under-doped high-temperature superconductors" and submitted in fulfillment of the requirements for the degree of Doctor of Philosophy in Physics complies with the regulations of the university and meets the accepted standards with respect to originality and quality.

Dated: March 2018.

Signed by the Examining Committee:

External Examiner: Dr. Sudip Chakraborty.

Sign.————————————-Date——————

Internal Examiner: Dr. Cherinet Amente

Sign.——————————————Date————————

Research Supervisors: Prof. P. Singh

Sign.————————————Date————-

Chair person of the department: Dr. Teshome Senbeta

Sign.—————————Date————

Chair of Department or Graduate Program Coordinator ————-

Addis Ababa University, March 2018

This thesis is dedicated to the memory of my brother, Dadi Dinegde.

Contents

List of Figures

List of Tables

Abstract

Superconductivity often emerges in the proximity of, or in competition with, symmetry-breaking ground states such as antiferromagnetism or charge density waves(CDW). A number of materials in the cuprate family, which includes the high transition-temperature(high-Tc) superconductors, show spin and charge density wave order. Thus a fundamental question is to what extent do these ordered states exist for compositions close to optimal for superconductivity. Recent observations of CDW order in $YBa_2Cu_3O_y$ and other cuprate families have raised interesting questions regarding the general role of charge modulations and the relation to superconductivity. It was studied that in the system $La_{2-x}Ba_xCuO_4$ SDW and CDW orders appear to be intertwined with a spatially-modulated superconductivity. Here by developing a model Hamiltonian and by using quantum field theory Green's function formalism, we obtain mathematical expressions for superconductivity order parameter(Δ), and charge density wave order parameter(W) in under-doped $YBa_2Cu_3O_y$. We plot the phase diagram of superconducting order parameter (Δ) against temperature(T) for different values of charge density wave orders(W) in under-doped $YBa_2Cu_3O_y$. The relationship between superconductivity(Δ), charge density wave(W), and spin density wave(M) orders and their critical temperatures is studied theoretically for the under-doped $La_{2-x}Ba_xCuO_4$ superconductor and plot the phase diagrams of superconducting order parameter(Δ) against temperature(T) for different values of charge density wave(W) and spin density wave(M) orders. Finally, we examine the physics of combined mechanisms for cuprates and pnictides.

Acknowledgement

This work would not have been possible without the help, guidance and support of many people.

I would like to express my gratitude, first and foremost, to my advisor P. Singh for his patient guidance, encouragement and excellent advice throughout this study.The decision to become his PhD. student was one of the best in my life. He was for me a great inspiration not only as a physicist but as well as a person.

Finally, I take this opportunity to express my profound gratitude to my beloved parents, my wife, my children, my brothers and sisters for their moral support and patience during my study.

I should not forget to thank to all my friends and others that inspired and supported me in any way.

Above all, I thank the Almighty God for all the blessings He has given me without which I could not have completed this long road to PhD.

Urga Dinegde

Addis Ababa University

March 2018

Ethiopia.

Chapter 1

Introduction

1.1 Introduction to Superconductivity

1.1.1 History of superconductivity

Superconductivity is a phenomenon of exactly zero electrical resistance and expulsion of magnetic fields occurring in certain materials when cooled below a characteristic critical temperature. Its special physical properties have attracted the attention of many physicists and electric engineers, since it was discovered by Dutch physicist Heike Kamerlingh Onnes in 1911. He and his co-workers cooled mercury to the boiling temperature of liquid helium ($4.2K$) and observed the abrupt vanishing of its electrical resistance[2] as shown in Fig 1.1 .

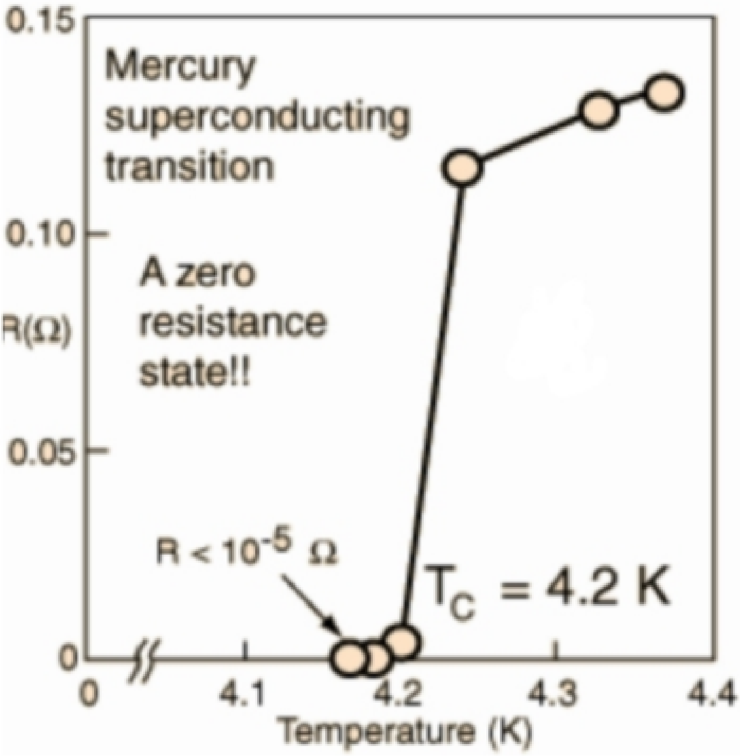

Figure 1.1: Experimental data obtained on mercury by Kamerling Onnes showing the superconducting transition for the first time.[1]

He was awarded the Nobel Prize in Physics for low temperature investigations in 1913. Since then, it has been a key interest to understand the mechanism behind superconductivity and find superconducting materials with higher Tc values. Physicists have considerable interest to study the variation of electrical resistivity with temperature.

The next great discovery in understanding superconductivity occurred when the expulsion of magnetic field was discovered by Meissner and Ochsenfeld in 1933 [3]. This phenomenon of superconductivity is now known as the Meissner effect. Over the next few decades, theorists struggled to find a microscopic theory for superconductivity. Major advances were made toward such a theory for superconductivity with the development of the London theory[4] in 1935 and the Ginzberg-Landau theory [5] in 1950. The complete microscopic theory of superconductivity was finally proposed in 1957 by Bardeen, Cooper, and Schrieffer[6] and is called the BCS theory. The authors were awarded the Nobel Prize in Physics in 1972 . In general, the BCS theory limits superconducting transition temperatures to below 30 K. The limiting value of Tc was calculated as a function of the electron-phonon and electron-electron coupling constants within the framework of the strong-coupling theory [7]. Indeed, no superconducting compounds with Tc values higher than $30K$ were known for a long time. In this context, the most important low-temperature superconductors are the metallic A15 compounds ($Nb_3Ge, Tc = 23K$)[8].

A genuine breakthrough was achieved in superconductivity research when high-temperature superconductivity was discovered in the cuprates in 1986 [9]. These ceramic superconductors show T_c higher than 77 K (the boiling point of liquid nitrogen), with 92 K in $YBa_2Cu_3O_7$ [10] . The highest confirmed value of T_c at ambient pressure so far is 133 K observed in $HgBa_2CaCu_2O_{6+x}$ [11]. In 1994, another class of superconductor, rare-earth borocarbides were discovered with a highest T_c of 23 K for YPd_2B_2C [12] . There was another surprise in the superconductor world when a metallic superconductivity with a Tc value of 39 K was found in a simple binary compound MgB_2 in 2001 [13]. In March 2008, a new era in superconductivity research began with the discovery of high-Tc superconductivity in an iron based compound with a Tc of 26 K [14]. Many families of Fe-based superconductors have been discovered within the last couple of years. To date, the maximum value of Tc found in the Fe-based superconductors is 56 K for $Gd_{1-x}Th_xFeAsO(x = 0.2)$ [15] . The discovery of high-Tc superconductivity in these Fe-based materials has emerged as a huge surprise to the scientific community, since the compound contain the most familiar ferromagnetic atom Fe and there is a historical antagonistic relationship between superconductivity and magnetism. This has opened a new path of research driven by the fact that our fundamental understanding of the origins of superconductivity needs significant improvement. A great deal of work is in progress around the world to explore the similarities of this new class of Fe-based superconductors with the cuprate superconductors and thereby pave the way towards understanding the superconducting mechanism behind these high temperature superconductors. The record of superconductivity pressurized hydrogen sulfide(H_2S) was reported in June 2015 with a maximum Tc onset of 203 K [23].

Fig 1.2 shows the superconducting critical temperature(Tc) of several high-Tc superconductors and metallic superconductors as a function of the year of discovery.

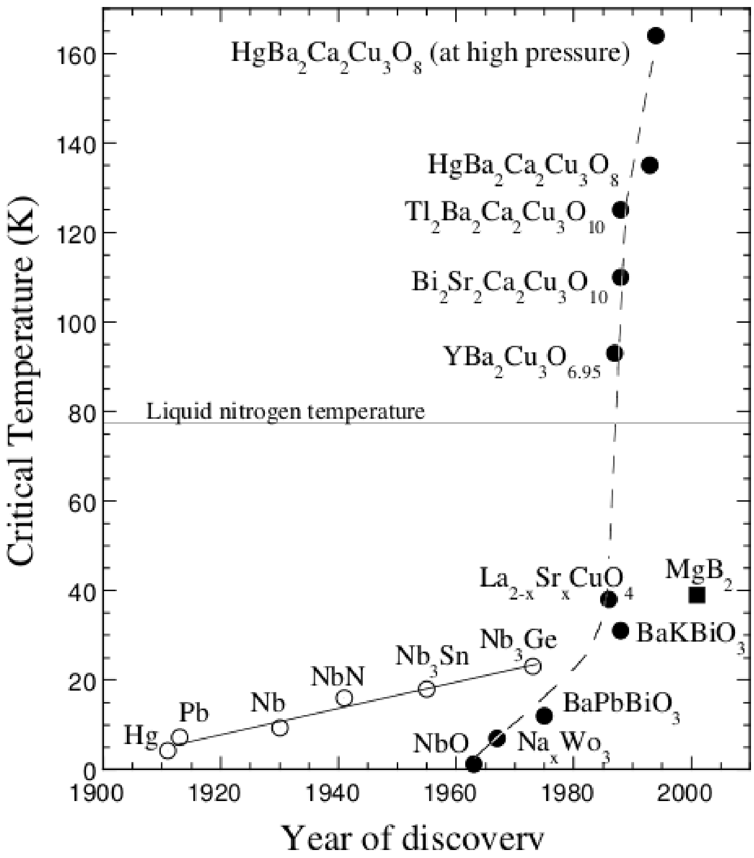

Figure 1.2: The time evolution of the superconducting critical temperature since the discovery of superconductivity in 1911.[122]

1.1.2 Types of superconductors

As scientists began to probe the exciting new properties of superconductors, they discovered that superconductors did have limitations apart from a maximum operating temperature. Although currents can flow without any energy dissipation, superconductivity is destroyed by the application of a sufficiently large magnetic field or if the flowing electrical current density exceeds a critical value.

The critical magnetic field depends on how far below the critical temperature the material is. Fig.1.3 given below shows this dependence. As more superconducting materials were discovered, it was found that they fell into one of two classes, or types with regard to their magnetic properties, and in particular in the way that they expelled magnetic fields. Type I superconductors have a sharp transition from the superconducting state where all magnetic flux is expelled to the normal state. Type I materials show at least some conductivity at ambient temperature and include mostly pure metals and metalloids. They have low critical temperatures, typically between 0 and 10 K (-273C and -263C respectively). As discussed above, this type experiences a sudden decrease in resistance as well as the complete expulsion of magnetic fields (perfectly diamagnetic) at critical temperature. The variation of the thermodynamic critical field H_c with temperature for a type-I superconductor is approximately parabolic [1]

$$H_c(T) \simeq H_c(0)(1 - (T/T_c)^2) \tag{1.1.1}$$

where $H_c(0)$ is the value of the critical field at absolute zero. The dependence $H_c(T)$ is schematically shown in Fig. 1.3 (left)

Most Type II materials are metallic compounds or alloys, although elemental vanadium, technetium, and niobium also fall within this group. They are capable of superconductivity at much higher critical temperatures. Type II materials also take on a mixed state, which contrasts with plunging resistance at Tc for Type I materials, when approaching their critical temperature. Mixed states are caused by the fact that Type II superconductors never completely expel magnetic fields, so that microscopic superconducting "stripes" can be seen on the material classification according to the types above is theoretically done by magnetic field behavior. Type I materials have a single critical field temperature above which superconductivity ceases completely, while Type II materials have two critical field points between which a mixed state may exist. For a type-II superconductor, there are two critical fields, the lower critical field H_{c1} and the upper critical field H_{c2} , as shown in Fig. 1.3 (right). In applied fields less than Hc1 , the superconductor completely expels the field, just as a type-I superconductor does below Hc . At fields just above H_{c1} , flux, however, begins to penetrate the superconductor in microscopic filaments called vortices which form a regular (triangular) lattice. Each vortex consists of a normal core in which the magnetic field is large, surrounded by a superconducting region, and can be approximated by a long cylinder with its axis parallel to the external magnetic field.

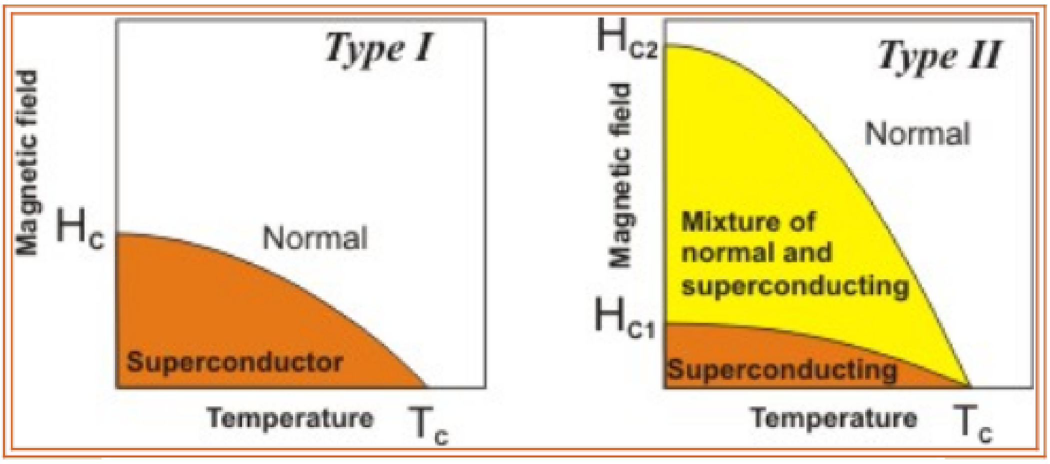

Figure 1.3: Schematic plot of magnetic field vs temperature of type-I(left) superconductor and type-II(right) superconductor.[1]

r

1.1.3 London Theory

London equation was developed by F. London and H. London in 1935 [16]. It was the first theory to explain the Meissner effect. Originally this theory was motivated by a two-fluid model for super-fluid ^3He, but the result could be utilized to account for the behavior of superconductors. Derived from the two-fluid model, London equation is given by

$$\vec{j_s} = -\frac{n_s e^2}{m_e}\vec{A} \tag{1.1.2}$$

where$\vec{A}$ is the vector potential.

$$\vec{B} = \nabla \times \vec{A} \tag{1.1.3}$$

where n_s , e, and m_e are the number density, the charge, and mass of superconducting electrons respectively electrons respectively, and $\vec{J}$ is the super-current density due to the applied field.

To find out its physical meaning, curl operator is applied on both sides of equation (1.1.2) and this yields

$$\nabla \times \vec{J_s} = \frac{n_s e^2}{m_e}\vec{B} \tag{1.1.4}$$

Now, use the Maxwell equation with static E-field, i.e.:

$$\nabla \times \vec{B} = \mu_0 \vec{J}_s \tag{1.1.5}$$

and substitute it into Equation (1.1.3), it becomes

$$\nabla \times (\nabla \times \vec{B}) = -\mu_0 \frac{n_s e^2}{m_e} \vec{B} \tag{1.1.6}$$

and rewriting it as

$$\nabla \times (\nabla \times \vec{B}) = -\frac{1}{\lambda^2} \vec{B} \tag{1.1.7}$$

Here λ is defined as London penetration depth which

$$\lambda = \sqrt{\frac{m_e}{\mu_0 n_s e^2}} \tag{1.1.8}$$

According to the identity

$$\nabla \times (\nabla \times \vec{B}) = \nabla(\nabla \cdot \vec{B}) - \nabla^2 \vec{B} \tag{1.1.9}$$

and the Maxwell equation

$$\nabla \cdot \vec{B} \tag{1.1.10}$$

we have Eq.(1.1.7) in the form of

$$\nabla^2 \vec{B} = \frac{1}{\lambda^2} \vec{B} \tag{1.1.11}$$

If B is along x-direction, where x represents the depth into body of the superconductor from the surface (x = 0), eq.(1.1.10) can be written as

$$\frac{d^2 \vec{B}}{dx^2} = \frac{1}{\lambda^2} B(\vec{x}) \tag{1.1.12}$$

Therefore,

$$B(z) = B(0)e^{\frac{-x}{\lambda}} \tag{1.1.13}$$

It indicates that the applied field will be screened out within the length of the penetration depth λ when the field enters the bulk superconductor. For $x >> \lambda$, there is no B-field inside the superconductor, which is exactly the Meissner effect. From this result, the physical meaning of λ is realized to be the length scale of the B-field penetrating into the superconductor. Typically λ is in the order of 100 nm. It implies that the field can only penetrate into a very thin layer on the surface, and practically almost all the region in the bulk of the superconductor has no B-field.

So the magnetic field does not drop abruptly at the superconductor surface but penetrates into the material with exponential attenuation as shown in Fig.1.4.

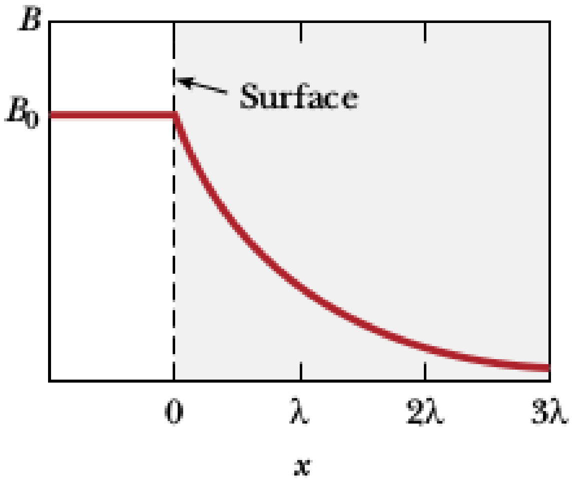

Figure 1.4: he magnetic field B inside a superconductor versus distance x from the surface of the superconductor. The field outside the superconductor (for $x < 0$) is B_0 , and the superconductor is to the right of the dashed line.[1]

We have now convinced ourselves that the superconductor can tolerate a magnetic field only in a thin surface layer (this is the case for type I superconductors). An immediate consequence is that current flow is restricted to the same thin layer.

1.1.4 BCS Theory

The first theory describing the superconducting phenomenon on a microscopic level was proposed by John Bardeen, Leon Neil Cooper, and John Robert Schrieffer in 1957, now a days being well-known as the BCS theory [28, 29]. This theory attempted to give a deep insight beyond the superconductivity itself by explaining the real nature of charge carriers transporting the electric current in superconductors on a quantum level. The main concept of this theory is in the electron pairing via crystal lattice vibrations (phonons) creating boson particles, which conduct an electric current without losses. Later on, these particles were named Cooper pairs, according to one of the BCS theory co-founders.

Let us assume an electron moving in a lattice cell containing positively charged atoms that vibrate at a characteristic frequency. The initial electron attracts surrounding atoms, which means that for a short time, electrostatic potential between the ions and the electron is changed. After that, the second electron, transferring through the changed potential, is attracted by the ions through the Coulomb force slightly more than the first electron, as attracted ions are not relaxed to their characteristic positions as shown in Fig.1.5. Therefore, it can be said that the first electron attracts the second electron through changed electrostatic potential at the particular place. The crucial fact for the pairing is a time difference between relaxation time of ions and time of the arrival of the second electron into changed potential. From a view point of quantum physics, these vibrations might be mathematically described by vibration quanta (phonons), and the pairing is mediated through the exchange of phonons.

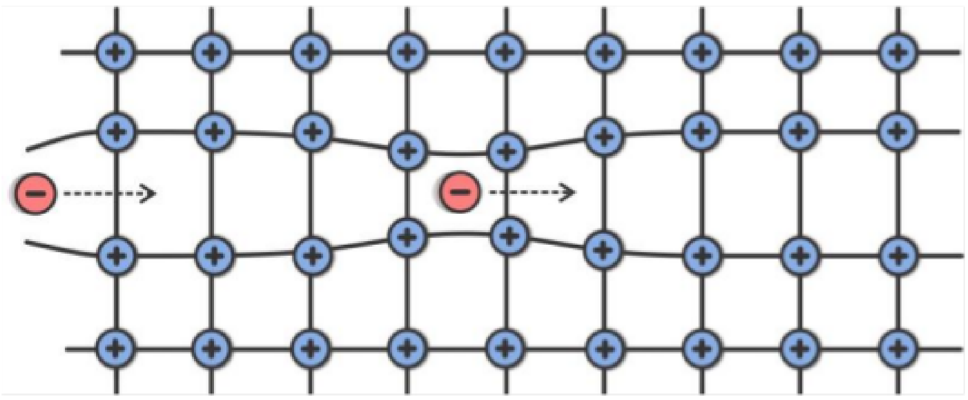

Figure 1.5: A schematic drawing of an electron interaction with crystal lattice ions.

The pairing interaction between two different electrons in states $(\vec{k}\uparrow)$ and $(-\vec{k}\downarrow)$ near the Fermi surface leads to creation of Cooper pairs. It can be pointed out that all Cooper pairs create one coherence state (at T=0), which can be expressed by one wave-function having quasi-macroscopic behavior.

BCS theory predicts the dependence of the value of the energy gap (Δ) at temperature T on the critical temperature Tc. Two times the energy gap is the binding energy of a Cooper pair (energy required to break the paired state), and the gap magnitude at zero temperature, $\Delta(0)$ is related to the superconducting transition temperature T by value[1]

$$2\Delta(0) = 3.52 k_B T_c \tag{1.1.14}$$

Near the critical temperature the relation asymptotes to [1]as shown in Fig 1.6

$$\Delta(T \to T_c) \approx 3.07 K_B T_c \sqrt{1 - (T/T_c)} \tag{1.1.15}$$

BCS theory relates the value of the critical field at zero temperature to the value of the transition temperature and the density of states at the Fermi level. In its simplest form, BCS gives the superconducting transition temperature Tc in terms of the electron-phonon coupling potential V and the Debye cutoff energy ω is given by [1]:

$$K_B T_c = 1.13 \hbar\omega \exp(-1/N(0)V) \tag{1.1.16}$$

where N(0) is the electronic density of states at the Fermi level. we assume weak coupling $N(0)V << 1$. A formula similar to eq(1.1.16) is predicted for the zero temperature energy gap: where k_B is the Boltzmann constant. At low temperature (below Tc, $k_B T$ is smaller than the gap and hence the superconducting electrons are not excited by the thermal vibrations of the lattice. The temperature dependence of the BCS energy gap shows that $\Delta(T)$ falls to zero at Tc [1]

$$\Delta(0) \approx 2\hbar\omega \exp(-1/N(0)V) \tag{1.1.17}$$

The essential result eq (1.1.17) shows that the energy gap at the temperature $T = 0K$ is proportional to the Debye frequency and the exponential factor$(\frac{-1}{N(0)V})$, which is given only by the density of electron states on the Fermi surface and the strength of electron-phonon interaction V. Higher density of electron states and stronger electron-phonon interaction lead to higher values of the energy gap (Δ). We can also find the ratio between the energy gap and the transition temperature as follows [1]

$$\frac{\Delta(0)}{K_B T_c} = 1.76 \tag{1.1.18}$$

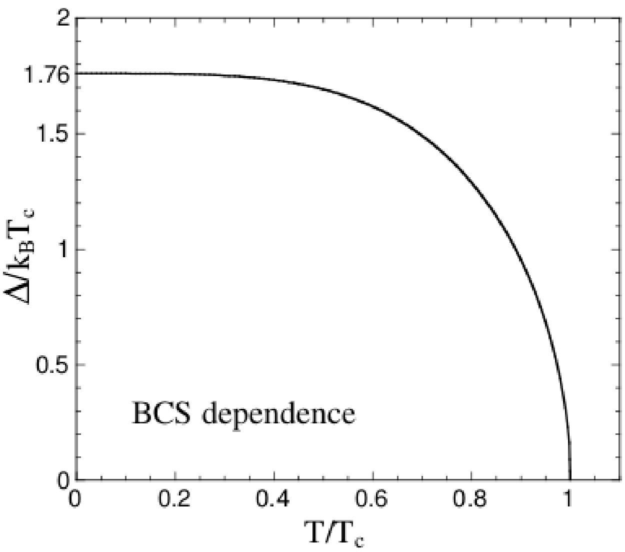

Figure 1.6: The BCS temperature dependence of the energy gap $\Delta(T)$.[1]

In the weak-coupling limit, i.e. when $\lambda \ll 1$, the influence of the Coulomb interaction on Tc in Eq.(1.1.16) can be taking into account by introducing the Coulomb pseudoptential [1]:

$$K_B T_c = 1.14\hbar\omega_D \exp(-\frac{1}{\lambda - \mu^*}) \tag{1.1.19}$$

where μ^* is N(0) times the Coulomb pseudo-potential. Later, McMillan extended this result for the case of strong-coupling superconductors, and obtained [1]

$$T_c = (\frac{\Theta_D}{1.45}) \exp[-\frac{1.014(1+\lambda)}{\lambda - \mu^*(1+0.62\lambda)}] \tag{1.1.20}$$

$$\lambda = 2\int_0^{\omega_D} \frac{\alpha^2(\omega)F(\omega)d\omega}{\omega} \tag{1.1.21}$$

where $\alpha(\omega)$ is the phonon coupling function and $F(\omega)$ is the phonon density of state,and Θ_D is the Debye temperature. The quantity λ is proportional to the static local compressibility of the lattice, which is independent of the isotope mass M since it is irrelevant to the ionic motion. Then where, apart from the parameter Θ, does the isotope effect come. In this formula μ represents the Coulomb pseudo-potential defined as [1]

$$\mu^* = \frac{N(0) < V_c >}{1 + N(0) < V_c > ln(\frac{\epsilon_f}{\Theta_D})} \tag{1.1.22}$$

where $< V_c >$ is the averaged Coulomb interaction. In an approximation of ignoring Θ_D dependence of μ^*, Tc is simply proportional to Θ_D and then proportional to $M^{-1/2}$. Therefore, the isotope exponent $\alpha \equiv \frac{-\partial(lnT_c)}{\partial(lnM)}$ becomes

$$\alpha = \frac{1}{a} \tag{1.1.23}$$

which is just the BCS result.

A superconductor with BCS gap symmetry is known to have s-wave pairing symmetry. In this pairing symmetry, electrons with opposite spin (singlet) form the cooper pairs. This is manifested as a finite-sized energy gap called superconducting gap in single particle excitations throughout the entire Fermi surface. Here, the orbital state of the Cooper pair can be a spherically symmetric analogous to an atomic s orbital.

The breaking of Cooper pairs is the mechanism by which the superconductivity is destroyed. This can occur by increasing the temperature so that the electrons can be thermally excited out of the state, but also by other pair-breaking mechanisms. For instance, the electrons are paired by $(\uparrow, \downarrow)$ and a magnetic field that would tend to align the spins along the direction of the field, $(\uparrow, \uparrow)$, say, would destroy the pairing. Magnetic impurities tend to spin-flip scatter the electrons as do spin-density fluctuations (paramagnons) and hence pairing is destroyed. Other pair-breaking effects can arise from an applied current which shifts the energies of the electrons and hence, large enough currents can give enough energy to the electrons to excite them out of the superconducting state. These are some of the pair-breaking mechanisms.

1.2 Basic properties of the superconducting state

A superconductor has several main macroscopic characteristics, such as: Zero Resistance , The Meissner Effect, The Josephson Effect , The Isotope Effect, Proximity effect, Anomalous Specific Heat Capacity etc. Here we will focus on four basic properties, namely zero resistance, Meissner Effect the Josephson Effect, and Proximity effect, Thermodynamic properties.

1.2.1 Zero resistance

The zero resistance characteristic of the superconductor refers to the phenomenon that resistance abruptly disappears at a certain temperature. It is able to transport direct current (DC) without resistance in the superconducting state.

The typically experimental dependence of resistance on temperature in a superconductor is shown in Fig 1.1, in which the resistivity of the superconductor suddenly falls to zero when the temperature reduces to a certain value below the critical temperature Tc .

1.2.2 Complete Diamagnetism Meissner Effect

When the superconductor is subjected to a magnetic field,in a non-superconducting state, the magnetic field can penetrate the superconductor and so the inner magnetic field is not zero in its normal state Fig.1.7(left). However, when the superconductor is in a superconducting state, the magnetic flux within is completely excluded from the superconductor, and the inner magnetic field is zero, that is, the superconductor is completely diamagnetic. This phenomenon is called the Meissner effect which was discovered by Walther Meissner and Robert Ochsenfeld in 1933. The superconductor can be suspended in a magnetic field due to its diamagnetism or the Meissner effect Fig.1.7(right)

We first explain such an effect in the context of classical electrodynamics. Since the resistivity (ρ) of superconductor is zero, the electric field $\vec{E}$ is also zero according to Ohm's law:

$$\vec{E} = \rho \vec{J} \tag{1.2.1}$$

where $\vec{J}$ is the current density. Applying it to the Faraday's law that

$$\nabla \times \vec{E} = -\frac{\partial \vec{B}}{\partial t} \tag{1.2.2}$$

it results in

$$\frac{\partial \vec{B}}{\partial t} = 0 \tag{1.2.3}$$

In the case of applying magnetic field after transforming to the superconducting state $\vec{B}$ is zero. However, if the happening sequence is reversed, $\vec{B}$ is not necessarily zero. Obviously, classical electrodynamics cannot explain the origin of Meissner effect. In other words, superconductor is not just a "perfect conductor". This special effect becomes another characteristic property of superconductors. In a magnetic medium,

$$\vec{B} = \mu_0(\vec{H} + \vec{M}) \tag{1.2.4}$$

where μ_0 is magnetic permeability in free space, $\vec{H}$ is the applied field, and $\vec{M}$ is the magnetization of the medium. When B is zero

$$\vec{H} = -\vec{M} \tag{1.2.5}$$

Therefore, superconductor is regarded as perfect diamagnetic material. As the diamagnetic effect is very strong, the magnetization drops sharply at Tc Since the measurement of magnetization is free of contact, the measurement of magnetization against temperature is also commonly used as a proof of superconductivity due to its convenience. Meissner found that no magnetic field is allowed inside a metal when it is in a superconducting state.

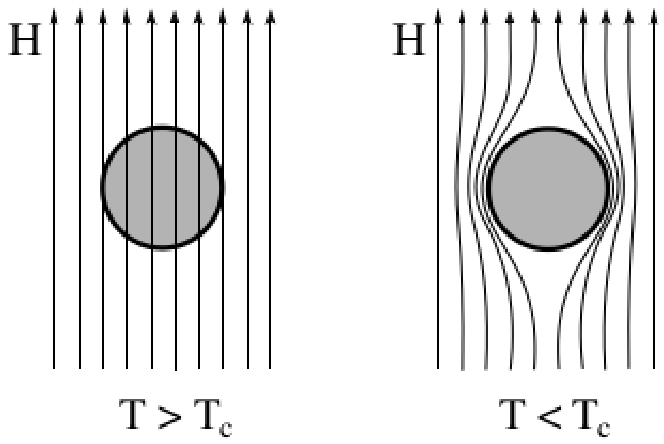

Figure 1.7: Diagram of the Meissner effect. Magnetic field lines, represented as arrows, are excluded from a superconductor when it is below its critical temperature.[1]

Probably, the most spectacular demonstration of the Meissner effect is the levitation effect. A small magnet above Tc simply rests on the surface of a superconductor having dimensions larger than those of the magnet. If the temperature is lowered below Tc , the magnet will float above the superconductor as shown in Fig 1.8. The gravitational force exerted on the magnet is compensated by the magnetic pressure occurring due to supercurrent circulation on the surface of the superconductor.

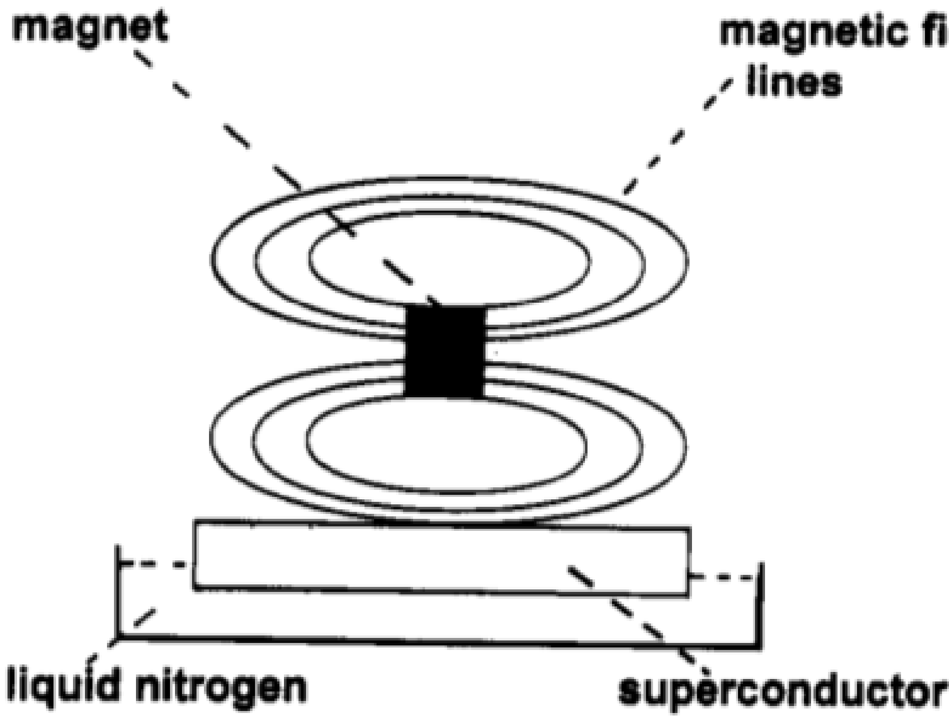

Figure 1.8: A magnet levitating over a superconductor. [1]

1.2.3 Isotope Effect in Conventional Superconductors

Isotope effect studies have been vital to the development of the microscopic theory of superconductivity. The first piece of evidence about the existence of isotope effect in mercury was reported in 1950 by Maxwell[17] and independently by Reynold et al.[18]. They found that the critical temperature Tc of mercury varies as an inverse function of isotopic mass. The argument that isotope mass enters into the formation of the superconducting phase implies that superconductivity is not purely electronic in origin. In the same year, Frohlich[19] proposed that same electron lattice interaction responsible for the scattering of conduction electrons by lattice vibrations provides a necessary glue between electrons. Frohlichs theory got a strong base from the experimental observation of isotope effect and played a key role in understanding microscopic mechanism of superconductivity.

Within the framework of BCS microscopic theory, one has relation between transition temperature Tc, typical phonon frequency ω (e.g Debye frequency) and interaction strength $N(0)V$

as[1]

$$K_BT_c = 1.14\hbar\omega \exp(-\frac{1}{VN_0}) \tag{1.2.6}$$

where V is the pairing potential arising from the electron phonon interaction, N(0) is the electronic density of states at Fermi surface and K_B is the Boltzmann constant. Equation (1.2.6) is considered as one of the most significant and influential prediction of BCS theory. In the harmonic approximation both V and N(0) are independent of the ionic mass, while characteristic frequency ωcan be expressed as[1]

$$\omega \propto \frac{1}{\sqrt{M}} \tag{1.2.7}$$

where M is the ionic mass.

1.2.4 Proximity effect

Every superconductor exhibits the proximity effect. The proximity effect occurs when a superconductor S is in contact with a normal metal N. If the contact between the superconductor and normal metal is of a sufficiently good quality, the order parameter of the superconductor close to the interface, Ψ , will be altered. The superconductor, however, does not react passively to this intrusion. Instead, it induces superconductivity into the metal which was in the normal state before the contact. Of course, this induced superconductivity exists only in a thin surface layer of the normal metal near the NS interface.

Thus, when a normal metal and a superconductor are in good contact, the Cooper pairs from the superconductor penetrate into the normal metal, and live there for some time. This results in the reduction of the Cooper-pair density in the superconductor. This also means that in a material which by itself is not a superconductor, one can, under certain conditions, induce the superconducting state. So, the proximity effect gives rise to induced superconductivity.

1.2.5 Thermodynamic properties

The transition from the normal state to the superconducting state is the second-order phase transition. Rutgers formula, that defines the height of the specific-heat jump at Tc in the framework of the BCS theory for conventional superconductors (the weak electron-phonon coupling approximation),this jump is given by[1].

$$\beta = \frac{\Delta C}{C_n} |_{T_c} = \frac{C_s - C_n}{C_n} = 1.45 \tag{1.2.8}$$

In the normal state, thus above Tc , the specific heat C_n linearly decreases as the temperature decreases, $C_n = \gamma T$, as shown in Fig.1.9. Such a linear dependence of specific heat is typical for normal metals, and represents the electronic specific heat. In the superconducting state, thus below Tc , the specific heat falls exponentially, as the temperature decreases:

$$C_s \propto exp(\frac{-\Delta(T)}{k_B T}) \tag{1.2.9}$$

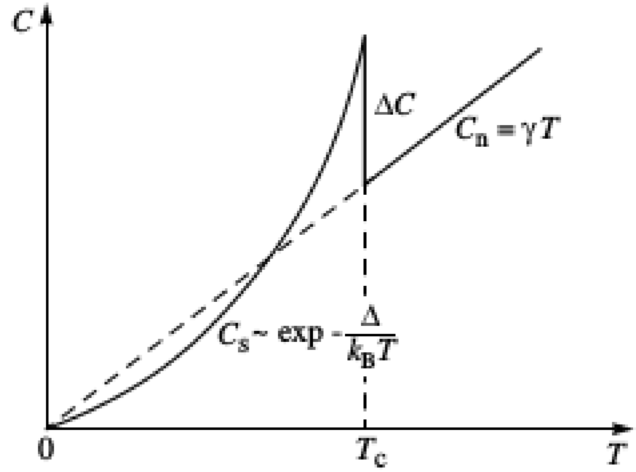

Figure 1.9: Temperature dependence of the specific heat of a superconductor. The characteristic jump ΔC occurs at Tc [1]

as schematically shown in Fig.1.9.

Out Line of the Thesis

This dissertation is organized as follows. In Chapter 2 the history of high-Tc copper based superconductor, Iron based superconductor is reviewed. Some crystal structures of high-Tc cuprates and high-Tc pnictides are described. Density waves and mechanisms of Cooper pairing in high-Tc superconductor is explained. In Chapter 3 the mathematical technique and formulation needed to solve our problem is discussed briefly. In Chapter 4 Competing Superconducting (Δ) and Charge-density Wave(W) Orders in underdoped $YBa_2Cu_3O_y$is discussed. In Chapter 5 Competing charge, spin, and superconducting orders in under-doped $La_{2-x}Ba_xCuO_4$ is discussed. In Chapter 6 Combined mechanisms of superconductivity is discussed. Finally we summarized the results.

Chapter 2

High Temperature Superconductivity

For some superconductors, the BCS theory cannot account for the physical properties. The observed critical temperatures are too high to be explained by the electron-phonon interaction. Some of families of such superconductors are the copper based superconductors and the iron based superconductors, since their critical temperatures are much higher than low temperature superconductors.

In 1986 Bednorz and Muller discovered superconductivity in a lanthanum based cuprate perovskite material, which had a transition temperature of 35 K. Lanthanum strontium cuprate oxide ($La_{2-x}Sr_xCuO_4$) discovered in the same year[49] . In Jan, 1987, Y BCuO was discovered with a superconducting transition temperature Tc = 92 K [50].

Recently, the highest temperature superconductor (at ambient pressure)is mercury barium calcium copper oxide ($HgBa_2Ca_2Cu_3O_x$), with Tc is 134 K[51] and reaches 164 K under high pressure [52].

In 2008, the highest T_c superconductor is pnictide ($Ca_{1x}Nd_xFeAsF$) with Tc = 57 K, was reported [53]

2.1 Cuprate Superconductors

The understanding of the superconductivity turned upside down when in 1986 J. G. Bednorz and K. A. Muller discovered that under certain conditions, layered copper oxide (cuprates) superconductor[9] . It was quite surprising that a very poor conductor could become a superconductor and the Tc was higher than any other known material. In less than one year after the discovery of superconductivity in cuprates, the effort of hundreds of labs around the world pushed the transition temperature above the liquid Nitrogen temperature (77K) with the discovery of $YBa_2Cu_3O_{7-x}$ (YBCO)[10].

Some cuprate superconductors are $YBa_2Cu_3O_{7-x}$ (YBCO), $Bi_2Sr_2CaCuO_{8+x}$ and $Bi_2Sr_2CuO_{6+x}$ (BSCCO), $La_{2-x}Sr_xCuO_4$ (LSCO), and $HgBa_xCuO_{4+x}$ (HBCO). Their common feature is the two dimensional CuO_2 planes in their structure. From angle-resolved photo-emission spectroscopy (ARPES)[37] and transport[38] experiments, as well as from band structure calculations[39, 14], it is established that cuprates are quasi two-dimensional (2D) conductors, and the electronic properties mostly originate from the d-orbital of copper and p orbital of oxygen in CuO_2 planes.

Superconductivity was observed in various compositions of cuprates and the table 2.1 summarizes the most studied compounds. Tc tends to increase for both increasing the number of neighboring Cu-O planes and reducing the disorder. This table also elegantly points out how structure effects, such as the dopant disorder, could influence the transition temperature. The only thing that all these high-Tc superconductors have in common is the presence of lightly doped copper-oxide (Cu-O) planes, that serves as the stage for all the physics that we are interested.

Table 2.1: Critical temperature (Tc), crystal structure and lattice constants of some high-Tc superconductors[122]

Formula	Notation	Tc (K)	No. of Cu-O planes in unit cell	Crystal structure
$YBa_2Cu_3O_7$	123	92	2	Orthorhombic
$Bi_2Sr_2CuO_6$	Bi-2201	20	1	Tetragonal
$Bi_2Sr_2CaCu_2O_8$	Bi-2212	85	2	Tetragonal
$Bi_2Sr_2Ca_2Cu_3O_{10}$	Bi-2223	110	3	Tetragonal
$Tl_2Ba_2CuO_6$	Tl-2201	80	1	Tetragonal
$Tl_2Ba_2CaCu_2O_8$	Tl-2212	108	2	Tetragonal
$Tl_2Ba_2Ca_2Cu_3O_{10}$	Tl-2223	125	3	Tetragonal
$TlBa_2Ca_3Cu_4O_{11}$	Tl-1234	122	4	Tetragonal
$HgBa_2CuO_4$	Hg-1201	94	1	Tetragonal
$HgBa_2CaCu_2O_6$	Hg-1212	128	2	Tetragonal
$HgBa_2Ca_2Cu_3O_8$	Hg-1223	134	3	Tetragonal

Phase diagram for cuprates superconductivity

A typical phase diagram of cuprate high-temperature superconductor is shown in Fig. 2.2, in which the phase of zero dopant concentration is anti-ferromagnetic (AF), and the doped carriers (electrons or holes) destroy the anti-ferromagnetic phase and induce superconductivity (SC). Hole doped cuprates present superconductivity when doping level is around $0.05 < x < 0.27$ where x is the hole doping per Cu in Cu-O planes. The doping level with x = 0.16 is optimal doping of which the Tc is maximum, and the doping level with $x < 0.16, x > 0.16$ are under-doped region,over doped region respectively.

In under-doped region, sample shows strange normal state that couldn't be described by conventional Fermi-Landau liquid theory which works quite well in the metals. For under-doped sample, an energy gap is opened above superconducting transition temperature Tc , and this gap is called pseudo-gap, while the energy gap is only opened below Tc in conventional superconductors. It is believed that clarifying the physics in under-doped region is indispensable in understanding the superconducting mechanism of cuprates, and whether the pseudo-gap state above Tc is a competitive phase of superconductivity or a precursor of superconductivity. In the normal state of over-doped region and the non superconducting region with doping level $x > 0.25$, the material presents characteristic of normal metal. For electron- doped region, the material presents anti-ferromagnetic in a wide doping region which is shown in Fig. 2.1, and only presents superconductivity in a narrow doping region.

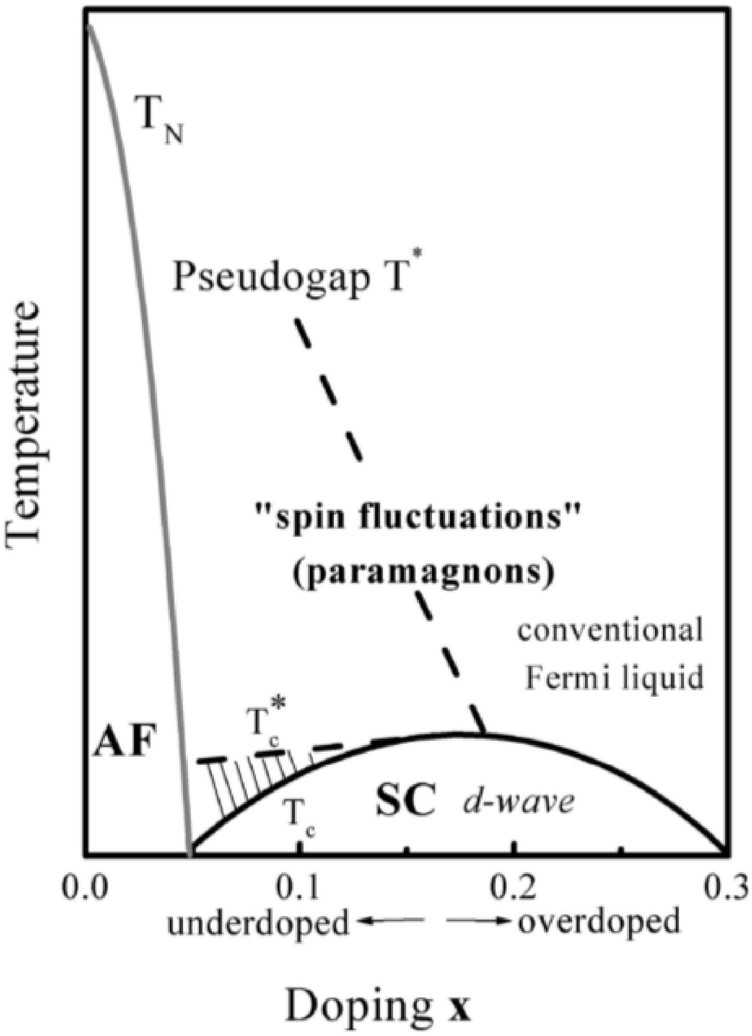

Figure 2.1: Phase diagram of hole-doped cuprates, showing superconductivity (SC), anti-ferromagnetic (AF), pseudogap, and normal-metal regions[122]

2.2 High Temperature Iron Based Superconductivity

For years the effect of high T_c superconductivity has been studied mainly in cuprate materials which has almost led to the conclusion that substantial copper content might be an obligatory condition for materials to exhibit high-temperature superconductivity. In 2008 this misconception was clearly disproved as Kamihara et al. discovered high-temperature superconductivity in a copper free material, $LaFeAsO_{1-x}F_x$ with-$Tc = 26K$ [40]. This finding, which immediately was followed by the discovery of superconductivity for a great number of other Fe-based superconducting materials, caused a lot of excitement in the community and propelled the field of high-Tc superconductivity, which at that time had slowed down a bit compared to the beginnings in 1986, back to be one of the most exciting fields in condensed matter physics again.

With the discovery by Kamihara et al. a real rush for new compositions with even higher critical temperatures was started and within a short span of time numerous discoveries were made. It was found that by replacing lanthanum in $LaFeAsO_{1-x}F_x$ by magnetic rare earths such as Ce, Sm, Nd or Pr the critical temperature could easily by increased up to 56 K[41, 42]. Simultaneously another class of Fe-based materials was discovered as Rotter et al. observed superconductivity with $Tc = 38K$ in $Ba_{0.6}K_{0.4}Fe_2As_2$ [43].

By now the field of Fe-based superconductors has been fully established and has become a very active field in solid state research with an uncountable number of scientific publications, a long list of international research groups working on a variety of different topics. Many different materials have been discovered with a range of different properties investigated with almost every experimental technique imaginable. The following sections will try to give a brief introduction to some of the basic properties of these Fe-based superconducting materials.

Structural Properties

Similar to the previously discussed cuprate materials, Fe-based superconductors crystallize in layered crystal structures. As illustrated in Fig.2.2 for the four main classes of Fe-based materials, these layered crystal structures are organized in an alternate stacking of Fe_2As_2 -layers and layers containing the other elements of the composition.

The shape of these tetrahedral surrounding the Fe-atoms in fact might impact the formation of the superconducting phase as it has been suggested that less distorted tetrahedral lead to higher critical temperatures[44]. As a result it was even proposed that the structural effects caused by doping might even be more important for the creation of superconductivity than the additional charge carriers provided by the introduction of foreign atoms to the system[45].

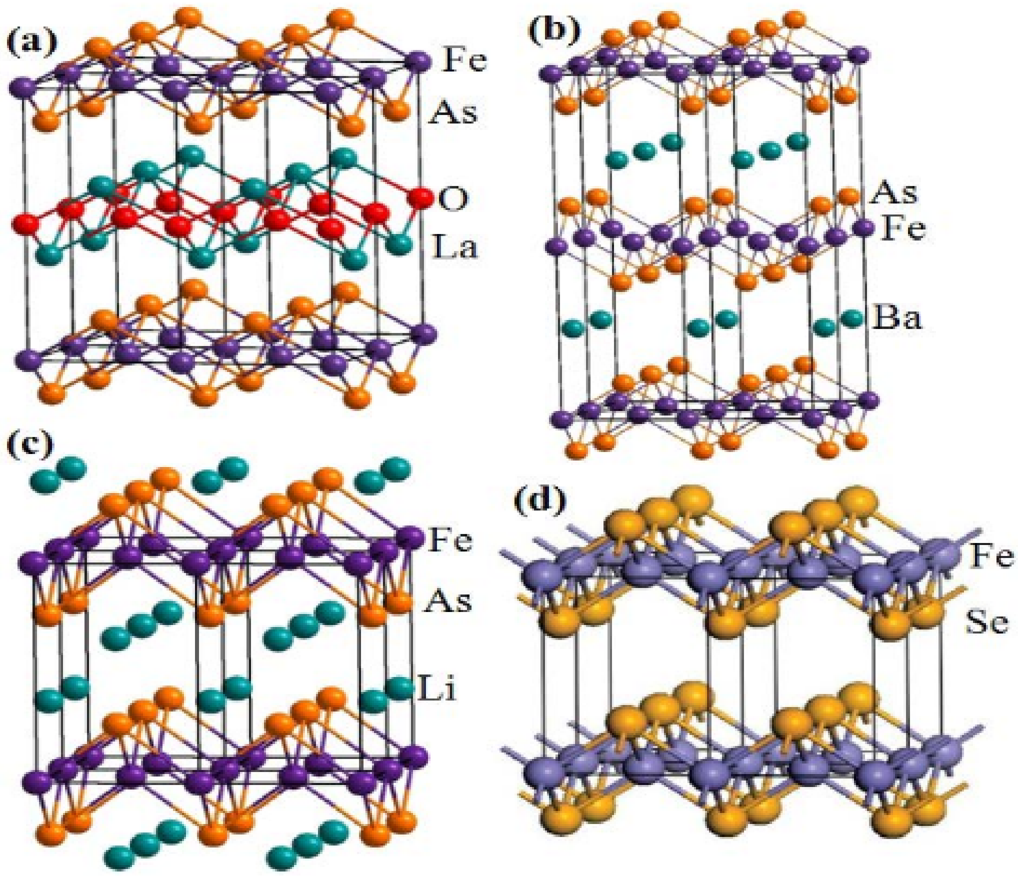

Figure 2.2: Four families of iron-based superconductors, (a) 1111, (b) 122, (c) 111, (d) 11 types [124]

The Phase Diagrams

Similar to the cuprates, all undoped Fe-based materials exhibit long range anti-ferromagnetic order, as in this case the Fe^{2+} moments form a magnetic sub-lattice. The magnetic order sets in after the crystal structure has transitioned from tetragonal to orthorhombic symmetry.

Doping the system with foreign atoms is one method to suppress the magnetic order and eventually induce superconductivity to the system. The doping can be conducted in several different ways, as basically all elements of the material can be replaced by foreign atoms. Depending of the introduction of these foreign atoms absorbs or emits electrons from or to the system the doping is referred to as either hole- or electron-doping. Increased doping concentration leads to a continuous suppression of the magnetic transition temperatures which is accompanied by a continuous reduction of the ordered magnetic moment and orthorhombic distortion of the crystal structure. As soon as the long range order is suppressed the system becomes superconducting, and aside for a small phase present in 122-materials the superconducting phase is related to a tetragonal crystal structure. For some 122-materials [46] and 1111-materials superconductivity even sets in before the magnetic order is completely suppressed, which leads to a coexistence of static magnetic order and superconductivity, and which clearly illustrates the compatibility of magnetism and superconductivity in these materials. The superconducting phase forms a dome-like shape in the phase diagram where the highest Tc is reached for a certain doping level (optimal doped), whereas both lower doping (under doped) and higher doping concentrations (over doped) lead to lower Tc and an eventual complete suppression of superconductivity as showing in Fig. 2.3.

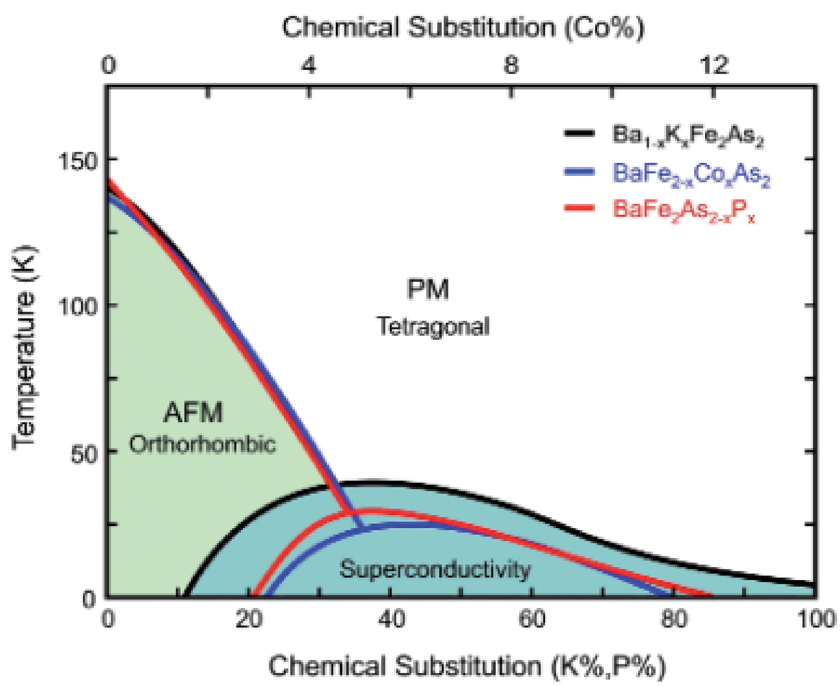

Figure 2.3: Phase diagram of iron-based superconducting systems derived from the $BaFe_2As_2$ parent compound,[124]

2.2.1 Iron-based superconductors versus Cuprate superconductors

Iron-based superconductors are usually compared with cuprate superconductors due to their similarity. Both of them are recognized to be unconventional superconductors due to their high-Tc behavior. They are also in layered structure with both superconducting layers and binding layers. In the cuprate compound, the superconducting layers are Cu-0 layers while the binding layers vary in different cuprate compounds. The most interestingly, their parent compounds are both antiferromagnetic.

They look very similar, but difference can still be found between them. Unlike iron-based materials, the parent compounds of cuprates are insulators. Upon doping, cuprate superconductors appear a phase called pseudo-gap phase, where an energy gap is present, between the anti-ferromagnetic phase and the superconducting phase .

2.3 Density Waves and High Temperature Superconductivity

Metals may undergo a phase transition to a state exhibiting a new type of electronic order upon cooling. A type of phase transition called charge density wave (CDW) state occurs in a class of metals with a chain crystal structure, namely, quasi-one-dimensional materials, as a consequence of electron-phonon interactions. The resulting state consists of a periodic charge density modulation accompanied by a periodic lattice distortion, both their periods being determined by the Fermi wave vector k_F. Consequently, both the electron and the phonon spectra are strongly modified by the formation of the CDW.

Rudolph Peierls [24] and H. Frohlich[4] independently suggested that a coupling of the electron and phonon systems in a one-dimensional metal is unstable with respect to a static lattice deformation of wave vector $Q = 2k_F$.

Below the Peierls transition temperature (T_P), CDW in one-dimension can simply be described as a periodic distortion of a quasi-one-dimensional lattice, which is accompanied by a periodic modulation of the electron density. A spin density wave (SDW) is closely related, and can be thought of as two CDWs for the spin-up and spin-down electrons that are 180^0 out-of-phase. Fig.2.4 illustrates a one-dimensional metal with lattice spacing a_0 distorted below the Peierls transition temperature T_P, introducing new periodicity $2a_0$, in to the lattice.

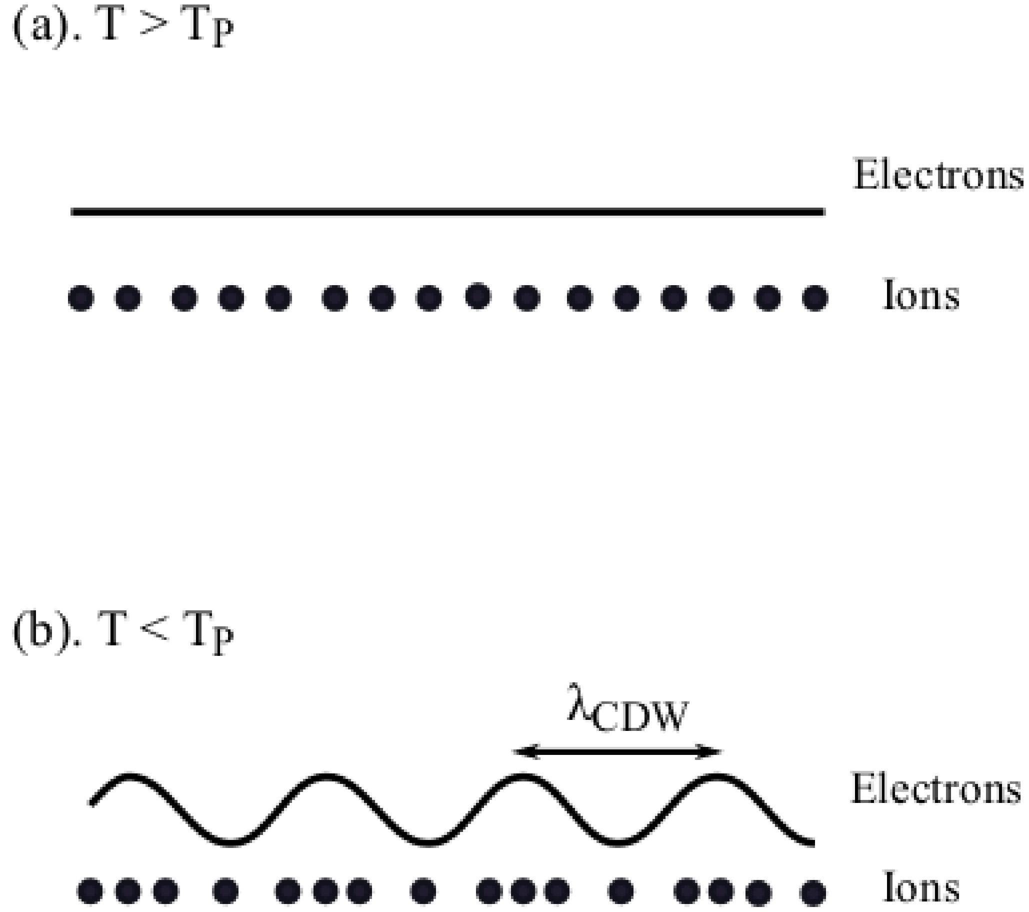

Figure 2.4: Formation of charge density wave (CDW) state in a one-dimensional metal. The dots represent the position of the metal ions and the solid lines represent the spatial variation of the charge density. (a)$T > T_P$ in the metallic state without the presence of CDW. The metal ions are evenly spaced and the electron charge density is uniform. (b) $T < T_P$ in the CDW state. The ions are displaced and electron density is periodically varying[125]

In 1955, Frohlich[25] demonstrated that the incommensurate CDW can slide through the lattice upon application of an infinitesimal electric field. Since the CDW carries charge collectively, it can contribute to electrical conductivity. Frohlich proposed this as a possible mechanism for superconductivity. Instead, the CDWs are not superconductors, since the CDW is usually pinned to the lattice by impurities and defects. Therefore, contrary to the Frohlich theory, the collective mode contribution to the electrical conductivity at low electric field is zero. However, if an moderate electric field is applied that is large enough to overcome the pining potential, the CDW is depinned from the underlying lattice and slides through the lattice. The sliding of the CDW results in increase of conductivity.

In general the order parameters interfere destructively; with CDW tending to suppress superconductivity and vice versa. A large enough CDW interaction which produces a semi conducting state may completely destroy superconductivity, but all metallic CDW states become superconductivity at sufficiently low temperature.

There are certainly many good examples of systems where the transition temperature for one type of order, such as charge density wave (CDW) or spin density wave (SDW) order, drops to zero at the same point where the superconducting Tc reaches its maximum. For example in $La_{2-x}Ba_xCuO_4$ SDW and CDW orders appear to be intertwined with superconductivity, referred to as a pair-density-wave (PDW) superconductor[69, 70].

Experimentally,it was studied that in the system $La_{2-x}Ba_xCuO_4$[68, 69, 70] SDW and CDW orders appear to be intertwined with a spatially-modulated superconductivity. Recently CDW order was observed in $YBa_2Cu_3O_{6+x}$[57, 61, 77] which competes with superconductivity.

2.4 Possible Mechanisms of Cooper Pairing in High-Tc Superconductivity

Till to date, a theory that completely describes High- Tc superconductivity continues to remain elusive. One reason for this is that the materials in question are generally very complex, multi-layered crystals, making theoretical modeling extremely difficult.

Most of the theories assume that polarization causes electron pairing. Two other things can be polarized is, charge or spin. A huge variety of exotic polarizing mechanisms excitons, plasmons, spin fluctuations have been proposed.

Combined phonon-exciton mechanism in copper based superconductors was proposed[104, 105, 106]. Singh et al. proposed bi-exciton as pairing mechanism for copper based superconductor [76]. Combined phonon-magnon mechanism in iron based superconductors was also proposed[89, 90].

Chapter 3

Mathematical Technique and Formulation

3.0.1 Green's function formalism

In this chapter we study double-time retarded Green's function technique given by Zubarev [20]. The Green's functions are the appropriate generalization of the concept of correlation functions and work as a propagator. In many body problems, determining properties of the system by solving the exact many body eigen function is very complicated. In such case and many others, the Green's function technique turns out to be simple, direct and very useful. In the situation of free field, as an example we shall deriving the corresponding statistical distribution functions under a basis set of general commutation relations which are suitable to not only the usual Bose and Fermi-statistics but the general one by using the double time Green's function technique in the first, second and third order decoupling approximations respectively.

In statistical mechanism different kinds of Green's functions are used. It is known that, the double Green's function describe the linear response of many body systems to external fields and treats quantum and thermodynamic fluctuations on the same level and it tightly related the correlation functions for describing the fluctuations. Therefore we believe that it is an effective approach to describing the statistical distribution function. In the present work double-time retarded greens functions are used. It is defined as follows:

$$G_r(t,t') = \langle\langle A(t), B(t')\rangle\rangle = -i\theta(t,t')\langle[A(t), B(t')]\rangle \tag{3.0.1}$$

where, $\hat{A}(t)$ and $\hat{B}(t')$ are the Heisenberg representation of operator$\hat{A}$ and $\hat{B}$, expressed in terms of a product of quantized field function (or of particle creation and annihilation operators). It is known that, $\hat{A(t)} = e^{i\hat{H}t}A(0)e^{-i\hat{H}t}$, $\hat{H}$ is Hamiltonian operator.

$$[\hat{A}, \hat{B}]_\eta = \hat{A}\hat{B} - \eta\hat{B}\hat{A},$$

where $\eta = +1$ for Bose operator and $\eta = -1$ for Fermi operator. And $\theta(t-t')$ is the Heaviside step function, defined as,

$$\theta(t-t') = 1, fort > t'$$

and

$$\theta(t-t') = 0, fort < t'$$

and $\langle.....\rangle$ denotes the thermal average and $\langle\langle.....\rangle\rangle$ is the abbreviated notation for the Green functions. The Heaviside step function related to the Dirac delta function as,

$$\frac{d}{dt}[\theta(t-t')] = \delta(t-t') \tag{3.0.2}$$

equation of motion for Green function is

$$i\frac{d}{dt}G_r(t-t') = \delta(t-t') < [\hat{A}(t), \hat{B}(t')] > +\langle\langle[\hat{A}(t), \hat{H}], \hat{B}(t')\rangle\rangle \tag{3.0.3}$$

for $t > t'$. The Fourier transformation $G_r(\omega)$is given by

$$G_r(t-t') = \int G_r(\omega)exp[-i\omega(t-t')]d\omega \tag{3.0.4}$$

Taking the Fourier transform of (3.0.3), we get:

$$\omega G_r(\omega) = \langle[\hat{A}(t), \hat{B}(t')]\rangle_\omega + \langle\langle[\hat{A}(t), \hat{H}], \hat{B}(t')\rangle\rangle_\omega \tag{3.0.5}$$

Finally we have

$$\omega\langle\langle\hat{A}(t), \hat{B}(t')\rangle\rangle_\omega = \langle[\hat{A}(t), \hat{B}(t')]\rangle + \langle\langle[\hat{A}(t), \hat{H}], \hat{B}(t')\rangle\rangle$$

Chapter 4

Competing Superconducting (Δ) and Charge-density Wave(W) Orders in underdoped $YBa_2Cu_3O_y$

Abstract

The relationship between the charge density wave (CDW) and superconductivity is a topic of interest in the research on the cuprate high T_c superconductors.

In this research work, the the interplay between charge density wave(CDW) and superconductivity in $YBa_2Cu_3O_y$ is studied. Starting with a model Hamiltonian for the system and using quantum field theory Green function formalism, we have found mathematical expressions for superconducting transition temperature Tc, charge density wave transition temperature (T_W), superconducting order parameter (Δ) and charge density wave order parameter (W). The phase diagrams of superconducting order parameter versus superconducting transition temperature , charge density wave order parameter versus and charge density wave transition temperature, and superconducting order parameter against temperature for different values of charge density waves are plotted.

Introduction

Charge-density-waves (CDW) have fascinated physicists for decades, since Peierls transition was suggested in one-dimensional metals coupled to an underlying lattice, where a periodic lattice distortion with wave vector $2k_F$ develops and results in opening up of a gap at the Fermi level[54, 55]. In a pioneering study, Lee, Rice, and Anderson [56] showed how fluctuations in the order parameter affect the CDW transition. They considered a model consisting of electrons in a linear chain coupled to phonons and predicted the appearance of a pseudogap in the CDW state that arises due to the thermal lattice motion.

The CDW state is a ubiquitous phenomenon in cuprate high-critical-temperature superconductors,appearing in the under-doped region in both hole-[57, 58, 59] and electron-doped[60] materials at a temperature higher than Tc, suggesting that the CDW is a characteristic instability of the CuO_2 plane. The CDW competes with superconductivity[57, 58, 59, 61], and pressure-dependent data[62] suggest that if the CDW can be suppressed in $YBa_2Cu_3O_y$ (YBCO), then an enhanced Tc occurs in the nominally under-doped region rather than at optimum doping. Experiments on YBCO using resonant soft X-ray scattering suggest that the CDW is associated with significant d-wave components for charges on the oxygen bonds around the Cu site [63, 64], as proposed by Sachdev[65].

The purpose of this work is to study theoretically how charge density wave order(W) and superconducting orders compete each other in under-doped $YBa_2Cu_3O_y$. Using the double time temperature dependent Greens function formalism we find the expression for superconducting order parameter(Δ) and charge density wave order(W) parameter. Within the framework of the BCS model, we propose the following model Hamiltonian (expressed in second quantized form), the the system as:

$$\hat{H} = \sum_{k\sigma} \epsilon_k c^\dagger_{k\sigma} c_{k\sigma} - \Delta \sum_{k\sigma} (c^\dagger_{k\uparrow} c^\dagger_{-k\downarrow} + h.c) - W \sum_{k\sigma} (c^\dagger_{k\sigma} c_{k+Q\sigma} + h.c) \tag{4.0.1}$$

The first term of $\hat{H}$ represent single particle energy of the conduction electron and the second term BCS type electron-electron pairing and the third term is charge density wave Hamiltonian; $(c^\dagger_{k\sigma}, c_{k\sigma})$ are the creation (annihilation) operators of an electron having the wave number k and spin σ, Q is the CDW vector,

$$\Delta = V\sum_k \langle\langle c_{k\uparrow}c_{-k\downarrow}\rangle\rangle = V\sum_k \langle\langle c^\dagger_{-k\downarrow}c^\dagger_{k\uparrow}\rangle\rangle \tag{4.0.2}$$

is defined to be superconducting order parameter; and is chosen real and positive.

$$W = \frac{U}{2}\sum_k \langle\langle c^\dagger_{k\sigma}c_{k+Q\sigma}\rangle\rangle$$

is the charge density wave order parameter. Inorder to derive an expression for superconducting order parameter Δ given in eq (4.0.2) we write equation of motion for $\langle\langle c_{k\uparrow}, c^\dagger_{k'\uparrow}\rangle\rangle$ which is

$$\omega\langle\langle c_{k\uparrow}, c^\dagger_{k'\uparrow}\rangle\rangle = \delta_{kk'} + \langle\langle [c_{k\uparrow}, \hat{H}], c^\dagger_{k'\uparrow}\rangle\rangle \tag{4.0.3}$$

Putting from eq (4.0,1) in eq (4.0.3)and applying anticomutation relation we get

$$(\omega - \epsilon_k)\langle\langle c_{k\uparrow}c^\dagger_{k\uparrow}\rangle\rangle = 1 - W\langle\langle c_{k+Q\uparrow}, c^\dagger_{k\uparrow}\rangle\rangle - \triangle\langle\langle c^\dagger_{-k\downarrow}c^\dagger_{k\uparrow}\rangle\rangle \tag{4.0.4}$$

The equation of motion for $\langle\langle c_{k+Q\uparrow}, c^\dagger_{k\uparrow}\rangle\rangle$ is

$$\omega\langle\langle c_{k+Q\uparrow}, c^\dagger_{k\uparrow}\rangle\rangle = \langle\langle [c_{k+Q\uparrow}, \hat{H}], c^\dagger_{k\uparrow}\rangle\rangle \tag{4.0.5}$$

simplifying we get

$$(\omega - \epsilon_{k+Q})\langle\langle c_{k+Q\uparrow}, c^\dagger_{k\uparrow}\rangle\rangle = -W\langle\langle c_{k\uparrow}, c^\dagger_{k\uparrow}\rangle\rangle \tag{4.0.6}$$

Similarly the equation of motion for $\langle\langle c^\dagger_{-k\downarrow}c^\dagger_{k\uparrow}\rangle\rangle$ can be written as

$$\omega\langle\langle c^\dagger_{-k\downarrow}, c^\dagger_{k\downarrow}\rangle\rangle = \langle\langle [c_{-k}, \hat{H}], c^\dagger_{k\uparrow}\rangle\rangle \tag{4.0.7}$$

and it gives

$$(\omega + \epsilon_{-k})\langle\langle c^\dagger_{-k\downarrow}c^\dagger_{k\uparrow}\rangle\rangle = -\Delta\langle\langle c_{k\uparrow}, c^\dagger_{k\uparrow}\rangle\rangle \tag{4.0.8}$$

Substituting eq(4.0.8) in eq(4.0.4) and simplifying we get

$$(\omega^2 - \epsilon_k^2 - \Delta^2)\langle\langle c^\dagger_{-k\downarrow}, c^\dagger_{k\uparrow}\rangle\rangle = -\Delta + \Delta W \langle\langle c_{k+Q\uparrow}, c^\dagger_{k\uparrow}\rangle\rangle \tag{4.0.9}$$

Putting eq(4.0.6) in eq(4.0.4) we get

$$(\omega^2 - \epsilon_k^2 - W^2)\langle\langle c_{k+Q\uparrow}, c^\dagger_{k\uparrow}\rangle\rangle = -W + \Delta W \langle\langle c^\dagger_{-k\downarrow}, c^\dagger_{k\uparrow}\rangle\rangle \tag{4.0.10}$$

Solving eq(4.0.9) and eq(4.0.10) simultaneously we obtain

$$\langle\langle c^\dagger_{-k\downarrow} c^\dagger_{k\uparrow}\rangle\rangle = \frac{-\Delta}{(\omega^2 - \epsilon_k^2 - \Delta^2 - W^2)} \tag{4.0.11}$$

And

$$\langle\langle c_{k+Q\uparrow} c^\dagger_{k\uparrow}\rangle\rangle = \frac{-W}{(\omega^2 - \epsilon_k^2 - \Delta^2 - W^2)} \tag{4.0.12}$$

Superconducting order parameter and transition temperature

In this section we calculate temperature dependence of superconducting parameter (Δ). The superconductivity order parameter (Δ) can be obtained using

$$\langle\langle c^\dagger_{-k\downarrow} c^\dagger_{k\uparrow}\rangle\rangle = \frac{-\Delta}{(\omega^2 - \epsilon_k^2 - \Delta^2 - W^2)}$$

Now the temperature dependence of superconducting order parameter can be written as:

$$\Delta = \frac{V}{\beta}\sum_k \langle\langle c^\dagger_{-k\downarrow}, c^\dagger_{k\uparrow}\rangle\rangle$$

where $\beta = \frac{1}{k_B T_c}$ and k_B is the Boltzmann constant. Then we can write

$$\Delta = \frac{V}{\beta}\sum_k \frac{-\Delta}{(\omega_n^2 - \epsilon_k^2 - \Delta^2 - W^2)} \tag{4.0.13}$$

We replace the summation by integration. Thus

$$\sum_k \equiv \int_{-\epsilon_f}^{\infty} N(0) d\epsilon \tag{4.0.14}$$

where $N(0)$is the density of states at the Fermi level. Substituting eq(4.0.14)in eq (4.0.13), we obtain,

$$1 = -\frac{VN(0)}{\beta} \int_{-\epsilon_f}^{\infty} \frac{d\epsilon}{(\omega^2 - \epsilon_k^2 - \Delta^2 - W^2)} \tag{4.0.15}$$

For further simplification, we use the Matsubara frequency $\omega \to i\omega_n$ where

$$\omega_n = \frac{(2n+1)\pi}{\beta} \tag{4.0.16}$$

Using (4.0. 16) and the fact that for effective pairing interactions,$-\hbar\omega < \epsilon < \hbar\omega$, we have from (4.0.15)

$$1 = 2VN(0)\beta \sum_n \int_0^{\hbar\omega} [\frac{1}{(2n+1)^2\pi^2 + \beta^2 E^2}] d\epsilon \tag{4.0.17}$$

where $E^2 = \Delta^2 + \epsilon_k^2 + W^2$. Finally, using the Poisson summation

$$\frac{1}{2x} tanh(\frac{x}{2}) = \sum_n \frac{1}{(2n+1)^2\pi^2 + x^2} = \frac{1}{2E\beta} tanh\frac{(E\beta)}{2} \tag{4.0.18}$$

where $x = E\beta$ and defining $\lambda = VN(0)$ which is electron-phonon constant eq(4.0.17) becomes

$$\frac{1}{\lambda} = \int_0^{\hbar\omega} \frac{tanh(\beta\sqrt{(\epsilon_k^2 + \Delta^2 + W^2})/2}{\sqrt{(\epsilon_k^2 + \Delta^2} + W^2)} d\epsilon \tag{4.0.19}$$

Right hand side of eq(4.0.19) can be written as

$$\int_0^{\hbar\omega} \frac{tanh(\beta\sqrt{(\epsilon_k^2 + \Delta^2 + W^2})/2d\epsilon}{\sqrt{(\epsilon^2 + \Delta^2 + W^2)}} = \int_0^{\hbar\omega} \frac{2}{\beta} \sum_{n=-\infty}^{n=\infty} \frac{1}{\omega_n^2 + \epsilon_k^2 + \Delta^2 + W^2} \tag{4.0.20}$$

$$\int_0^{\hbar\omega} \frac{2}{\beta} \sum_{n=-\infty}^{n=\infty} \frac{1}{\omega_n^2 + \epsilon_k^2 + \Delta^2 + W^2} = \int_0^{\hbar\omega} \frac{2}{\beta} d\epsilon \sum_{n=-\infty}^{n=\infty} \frac{1}{(\omega_n^2 + \epsilon^2)} - \int_0^{\hbar\omega} (W^2 + \Delta^2) d\epsilon \frac{2}{\beta} \sum_{n=-\infty}^{n=\infty} \frac{1}{(\omega_n^2 + \epsilon^2)^2} + ... \tag{4.0.21}$$

Using Laplaces transform and Matsubara frequency ,$\omega_n = \frac{(2n+1)\pi}{\beta}$ eq(4.0.20) can be written as

$$\frac{1}{\lambda} = \int_0^{\hbar\omega} \frac{tanh\beta\epsilon/2d\epsilon}{\epsilon} - (W^2 + \Delta^2)\int_0^{\hbar\omega} d\epsilon \frac{2}{\beta} \sum_{n=-\infty}^{n=\infty} \frac{1}{((2n+1)\frac{\pi}{\beta})^2 + \epsilon^2)^2}. \tag{4.0.22}$$

It is known that

$$\sum_{n=-\infty}^{n=+\infty} \frac{1}{(((2n+1)\frac{\pi}{\beta})^2 + \epsilon^2)^2} = 2\sum_{n=0}^{n=+\infty} \frac{1}{(((2n+1)\frac{\pi}{\beta})^2 + \epsilon^2)^2}$$

By using the relation

$$2\sum_{n=0}^{n=+\infty} \frac{1}{(a^2 + \epsilon^2)^2} = 2\sum_{n=0}^{n=\infty} \frac{1}{a^4(1 + \frac{\epsilon^2}{a^2})^2} = 2\sum_{n=0}^{n=\infty} \frac{1}{a^4(1 + x^2)^2}$$

where $x = \frac{\epsilon}{a}$, and $a = \frac{1}{(2n+1)\frac{\pi}{\beta}}$. Now the right hand side of eq (4.0.22)can be written as

$$\int_0^{\hbar\omega} \frac{tanh\beta\epsilon/2d\epsilon}{\epsilon} - (W^2 + \Delta^2)\int_0^{\hbar\omega} d\epsilon \frac{4}{\beta} \sum_{n=0}^{n=\infty} \frac{1}{a^4(1 + x^2)^2} + ... = p + q. \tag{4.0.23}$$

Where

$$p = \int_0^{\hbar\omega} \frac{tanh\beta\epsilon/2d\epsilon}{\epsilon}, q = (\Delta^2 + W^2)\int_0^{\hbar\omega} d\epsilon \frac{4}{\beta} \sum_{n=0}^{n=\infty} \frac{1}{a^4(1 + x^2)^2} + ...$$

Inorder to solve for p, let $y = \frac{\beta}{2}\epsilon$. Then

$$p = \int_0^{\beta\hbar\omega/2} \frac{tanhy}{y} dy = lnytanhy - \int_0^{\beta\hbar\omega/2} lnysech^2ydy \tag{4.0.24}$$

For $\frac{\hbar\omega}{2k_BT_c} >> 1, tanh\frac{\hbar\omega}{2k_BT_c} \to 1$. Extending the upper limit of the above equation we obtain

$$\int_0^{\infty} lnysech^2dy = ln\frac{\pi}{4\gamma,}$$

where $\gamma = exp(0.577)$. Now eq(4.0.24) becomes

$$p = ln\frac{\hbar\omega}{2k_BT} - ln\frac{\pi}{4\gamma} = ln1.14\frac{\hbar\omega}{k_BT} \tag{4.0.25}$$

Similarly we can solve for y as follows

$$q=(\Delta^2+W^2)\int_o^{\hbar\omega}d\epsilon\frac{4}{\beta}\sum_{n=0}^{n=\infty}\frac{1}{a^4(1+x^2)^2}=4(\Delta^2+W^2)\sum_0^{\infty}(\frac{\beta}{\pi(2n+1)})_2\int_0^{\infty}\frac{1}{(1+x^2)^2}dx+.. \tag{4.0.26}$$

$$=(\Delta^2+W^2)\frac{1}{(k_BT)^2}\frac{11}{100}$$

From standard integral we used $\int_0^{\infty}\frac{dx}{(1+x^2)^2}=\frac{\pi}{4}$ and $\sum_0^{\infty}\frac{1}{(2n+1)^2}=(1-2^{-r})\zeta(r)$ where $r=3,\zeta(r)=1.202$ it is called the Riemann Zeta function. By substituting eq (4.0.25) and eq (4.0.26) in eq (4.0.22)we obtain

$$\frac{1}{\lambda}=ln(1.14\frac{\hbar\omega}{K_BT})-1.05(\Delta^2+W^2)\frac{1}{(\pi k_BT)^2}. \tag{4.0.27}$$

From eq (4.0.27)the superconducting order parameter can be expressed interms of charge density wave parameter as

$$\Delta=\sqrt{[ln(1.14\frac{\hbar\omega}{k_BT})-\frac{1}{\lambda}]\frac{(\pi k_BT)^2}{1.05}-W^2} \tag{4.0.28}$$

As can be observed from eq(4.0.28) as charge density order parameter increases superconducting ordeder parameter is getting supressed as clearly shown in phase diagram fig (4.2). In pure superconducting phase where $W=0$, at Tc we have

$$\frac{1}{\lambda}=ln(1.14\frac{\hbar\omega}{K_BT_c}) \tag{4.0.29}$$

from which we can calculate

$$K_BT_c=1.14\hbar\omega\exp(-\frac{1}{\lambda})$$

which is the well known BCS expression for the superconducting transition temperature(T_c). Now lets consider the case as

$$T\to 0,\beta\to\infty$$

then from eq(4.0.19) we have

$$\frac{1}{\lambda}=\int_0^{\hbar\omega}\frac{d\epsilon}{\sqrt{(\epsilon_k^2+\Delta^2+W^2)}}$$

Simplifying the above expression we obtain

$$\sqrt{(\Delta^2 + W^2)} = 2\hbar\omega \exp(-\frac{1}{\lambda}) \tag{4.0.30}$$

This equation tells us that superconductivity and charge density wave can coexist in some region. From eq(4.0.30) superconductive order (Δ) as $T \longrightarrow 0$ can be expressed as

$$\Delta(0) = \sqrt{[2\hbar\omega \exp(\frac{-1}{\lambda})]^2 - W^2)} \tag{4.0.31}$$

When the charge density wave ordering (W) is absent the above equation reduces to

$$\Delta(0) = 2\hbar\omega \exp(-\frac{1}{\lambda})$$

From the BCS theory we have,

$$\frac{2\Delta(0)}{k_B T_c} = 3.5.$$

From which we get

$$k_B T_c = 1.14\hbar\omega \exp(-\frac{1}{\lambda})$$

which is the well known BCS expression for the superconducting transition temperature(T_c).

Order parameter in pure superconducting region

In pure superconducing region the charge density wave parameter where $W = 0$, from eq (4.0.19) we have:

$$\frac{1}{\lambda} = \int_0^{\hbar\omega} \frac{tanh(\beta\sqrt{(\epsilon_k^2 + \Delta^2)}/2)d\epsilon}{\sqrt{(\epsilon_k^2 + \Delta^2)}} \tag{4.0.32}$$

eq(4.0.32) can be transformed by using the technique of Laplace transformation

$$\frac{1}{\lambda} = \int_0^{\hbar\omega} d\epsilon \frac{2}{\beta} \sum_{n=-\infty}^{n=\infty} \frac{1}{\omega_n^2 + \epsilon^2} - \int_0^{\hbar\omega} d\epsilon \Delta^2 \frac{2}{\beta} \sum_{n=-\infty}^{n=\infty} \frac{1}{(\omega_n^2 + \epsilon^2)^2} + ..., \tag{4.0.33}$$

substituting the value of the Matsubra frequency

$$\omega_n = \frac{(2n+1)\pi}{\beta}$$

,then eq (4.0.33) becomes

$$\frac{1}{\lambda} = \int_0^{\hbar\omega} d\epsilon \frac{tanh\beta\epsilon_k/2}{\epsilon_k} - \int_0^{\hbar\omega} d\epsilon\Delta^2 \frac{2}{\beta} \sum_{n=-\infty}^{n=\infty} \frac{1}{(\frac{\pi(2n+1)}{\beta})^2 + \epsilon^2)^2} + ... \tag{4.0.34}$$

Simplifying eq(4.0.34) becomes

$$\frac{1}{\lambda} = ln(1.14\beta\hbar\omega) - 1.05\Delta^2 \frac{1}{(\pi k_B T_c)^2} \tag{4.0.35}$$

Using eq (4.0.29) in eq(4.0.35)we obtain

$$ln 1.14 \frac{\hbar\omega}{k_B T_c} = ln 1.14 \frac{\hbar\omega}{k_B T} - 1.05\Delta^2 \frac{1}{(\pi k_B T_c)^2} \tag{4.0.36}$$

From which we obtain

$$ln(\frac{T}{T_c}) = -1.05\Delta^2 \frac{1}{(\pi k_B T_c)^2} \tag{4.0.37}$$

This can be written as

$$ln(1 - (1 - \frac{T}{T_c})) = -1.05\Delta^2 \frac{1}{(\pi k_B T_c)^2} \tag{4.0.38}$$

Using the relation

$$ln(1 - (1 - y)) = -(1 - y) - \frac{(1 - y)^2}{2} \tag{4.0.39}$$

From which we obtain

$$\Delta(T) = 3.06 k_B T_c (1 - \frac{T}{Tc})^{1/2} \tag{4.0.40}$$

As can be seen from eq (4.0.40) that superconducting order parameter varies with temperature, it attains the maximum vlue at T=0 , decreases as temperature increasing and finally becomes zero at superconducting transition temperature Tc.

4.0.2 The Charge Density Wave(CDW) Parameter(W)

In this section we obtain the expression for charge density wave order parameter and discuss how it compete with superconductivity. To do so we write down the equation of motion for

$$\langle\langle c^{\dagger}_{k\sigma} c_{k+Q\sigma}\rangle\rangle.$$

Here we defined ($\sigma =\uparrow$). Using eq (4.0.1),the equation of motion for $\langle\langle c^{\dagger}_{k\uparrow} c_{k+Q\uparrow}\rangle\rangle$ is

$$\langle\langle c^{\dagger}_{k\uparrow} c_{k+Q\uparrow}\rangle\rangle = \langle\langle [c^{\dagger}_{k\uparrow}, \hat{H}], c_{k+Q\uparrow}\rangle\rangle \tag{4.0.41}$$

Simplifying eq(4.0.41) we get

$$(\omega + \epsilon_k)\langle\langle c^{\dagger}_{k\uparrow}, c_{k+Q\uparrow}\rangle\rangle = W\langle\langle c^{\dagger}_{k+Q\uparrow} c_{k+Q\uparrow}\rangle\rangle + \Delta\langle\langle c_{-k\downarrow} c_{k+Q\uparrow}\rangle\rangle \tag{4.0.42}$$

The equation of motion for $\langle\langle c^{\dagger}_{k+Q\uparrow}, c_{k+Q\uparrow}\rangle\rangle$ is

$$\langle\langle c^{\dagger}_{k+Q\uparrow}, c_{k+Q\uparrow}\rangle\rangle = 1 + \langle\langle [c^{\dagger}_{k+Q\uparrow}, \hat{H}], c_{k+Q\uparrow}\rangle\rangle \tag{4.0.43}$$

Simplifying this we get

$$(\omega + \epsilon_{k+Q\uparrow})\langle\langle c^{\dagger}_{k+Q\uparrow}, c_{k+Q\uparrow}\rangle\rangle = 1 + W\langle\langle c^{\dagger}_{k\uparrow} c_{k+Q\uparrow}\rangle\rangle \tag{4.0.44}$$

Similarly the equation of motion for $\langle\langle c_{-k\downarrow}, c_{k+Q\uparrow}\rangle\rangle$ is

$$\langle\langle c_{-k\downarrow}, c_{k+Q\uparrow}\rangle\rangle = \langle\langle [c_{-k\downarrow}, \hat{H}], c_{k+Q\uparrow}\rangle\rangle \tag{4.0.45}$$

Simplifying this equation we get

$$(\omega - \epsilon_{-k})\langle\langle c_{-k\downarrow} c_{k+Q\uparrow}\rangle\rangle = \Delta\langle\langle c^{\dagger}_{k\uparrow}, c_{k+Q\uparrow}\rangle\rangle \tag{4.0.46}$$

Substituting eq (4.0.46) in eq(4.0.42) and simplifying we get

$$(\omega^2 - \epsilon_k^2 - \Delta^2)\langle\langle c_{k\uparrow}^\dagger c_{k+Q\uparrow}\rangle\rangle = (\omega - \epsilon_k) W \langle\langle c_{k+Q\uparrow}^\dagger c_{k+Q\uparrow}\rangle\rangle \tag{4.0.47}$$

Finally solving eqs. (4.0.47) and (4.0.44)simultaneously and solving for $\langle\langle c_{k\uparrow}^\dagger c_{k+Q\uparrow}\rangle\rangle$ we get

$$\langle\langle c_{k\uparrow}^\dagger c_{k+Q\uparrow}\rangle\rangle = \frac{W}{(\omega^2 - \epsilon_k^2 - \Delta^2 - W^2)} \tag{4.0.48}$$

But the CDW order Parameter W is :

$$W = \frac{U}{2}\sum_k \langle\langle c_{k\uparrow}^\dagger c_{k+Q\uparrow}\rangle\rangle \tag{4.0.49}$$

The tempreture dependence of charge density wave parameter can be written as

$$W = \frac{U}{2\beta}\sum_k \frac{W}{(\omega^2 - \epsilon_k^2 - \Delta^2 - W^2)} \tag{4.0.50}$$

From eq(4.0.50) and eq(4.0.13) it is observed that

$$\Delta = f(\Delta, W)$$

and

$$W = f(\Delta, W).$$

This means in certain temperature interval superconductivity and charge density wave may co-exist. For mathematical convenience, we replace the summation by integration. Thus

$$\sum_k \equiv \int_{-\epsilon_f}^{\infty} N(0) d\epsilon \tag{4.0.51}$$

where $N(0)$is the density of states at the Fermi level. Substituting eq (4.0.51)in eq (4.0.50), we obtain,

$$1 = \frac{UN(0)}{2\beta}\int_{-\epsilon_f}^{\infty} \frac{d\epsilon}{(\omega^2 - \epsilon_k^2 - \Delta^2 - W^2)} \tag{4.0.52}$$

For further simplification, we use the Matsubara frequency $\omega \rightarrow i\omega_n$ where

$$\omega_n = \frac{(2n+1)\pi}{\beta} \tag{4.0.53}$$

Using eq(4.0.53) in eq (4.0.52) and the fact that for effective pairing interactions,$-\hbar\omega < \epsilon < \hbar\omega$ we have

$$1 = UN(0)\beta \sum_n \int_0^{\hbar\omega} [\frac{1}{(2n+1)^2\pi^2 + \beta^2 E^2}] d\epsilon \tag{4.0.54}$$

where $E^2 = \Delta^2 + \epsilon_k^2 + W^2$. Finally, using the Poisson summation

$$\frac{1}{2x} tanh(\frac{x}{2}) = \sum_n \frac{1}{(2n+1)^2\pi^2 + x^2} = \frac{1}{2E\beta} tanh\frac{(E\beta)}{2}, \tag{4.0.55}$$

where $x = E\beta$. Using eq(4.0.55) , eq (4.0.54) can be written as

$$\frac{1}{\chi} = \int_0^{\hbar\omega} \frac{tanh(\frac{\beta E}{2})}{2\beta E} d\epsilon \tag{4.0.56}$$

where we used $\chi = N(0)U$ is charge density wave coupling constant. Eq (4.0.54) can be written as

$$\frac{-1}{\chi} = \int_0^{\hbar\omega} d\epsilon \frac{tanh\frac{\beta}{2}\sqrt{(\Delta^2 + \epsilon^2 + W^2)}}{2\sqrt{(\Delta^2 + \epsilon^2 + W^2)}} \tag{4.0.57}$$

We solved eq(4.0.57) using same procedure we used to solve for the superconducting order parameter described in eq (4.0.20)to eq (4.0.27) ,we can get the expression for the charge density wave order parameter as

$$-\frac{1}{\chi} = ln(1.14\frac{\hbar\omega}{K_B T}) - 1.05(\Delta^2 + W^2)\frac{1}{(\pi k_B T)^2}. \tag{4.0.58}$$

From eq(4.0.58)the charge density wave order parameter(W) can be expressed in terms of superconducting order parameter as

$$W = \sqrt{[ln(1.14\frac{\hbar\omega}{k_B T}) + \frac{1}{\chi}]\frac{(\pi k_B T)^2}{1.05} - \Delta^2} \tag{4.0.59}$$

Again from eq (4.0.59) it is clear that as superconducting parameter increases the charge order parameter getting suppressed as is plotted in phase diagram in Fig (4.4). From eq(4.0.28)and eq (4.0.59) it is clear that superconducting and charge density wave orders are comepeting each other.

As $T \to T_W$,$W \to 0$. Then eq (4.0.57) can be written as

$$\frac{-2}{\chi} = \int_0^{\hbar\omega} d\epsilon \frac{tanh\frac{\beta}{2}\sqrt{(\Delta^2+\epsilon^2)}}{\sqrt{(\Delta^2+\epsilon^2)}} \tag{4.0.60}$$

Using the Laplace ttransformation, eq (4.0.60)becomes

$$\frac{-2}{\chi} = \int_0^{\hbar\omega} \frac{d\epsilon tanh\beta\epsilon_k/2}{\epsilon_k} - 2\beta^3\Delta^2 \int_0^{\hbar\omega} d\epsilon \sum_{n=-\infty}^{n=\infty} \frac{1}{(\pi(2n+1))^4(1+\frac{(\beta\epsilon)}{\pi(2n+1)})^2} \tag{4.0.61}$$

from which we get

$$\frac{-2}{\chi} = ln1.14\frac{\hbar\omega}{K_BT_W} - 1.05\Delta^2\frac{1}{(\pi k_BT_W)^2} \tag{4.0.62}$$

Since Δ is small enough we can neglect Δ^2 term, eq (4.0.62)becomes

$$\frac{-2}{\chi} = ln(1.14\frac{\hbar\omega}{k_BT_W}) \tag{4.0.63}$$

In pure CDW phase $\Delta = 0$ eq (4.0.57) becomes

$$\frac{-2}{\chi} = \int_0^{\hbar\omega} d\epsilon \frac{tanh\frac{\beta}{2}\sqrt{\epsilon^2+W^2)}}{\sqrt{\epsilon^2+W^2)}} \tag{4.0.64}$$

and simplifying it as usual we obtain

$$\frac{-2}{\chi} = ln1.14\frac{\hbar\omega}{k_BT} - 1.05W^2\frac{1}{(\pi k_BT_W)^2} \tag{4.0.65}$$

Comparing eq (4.0.65) and eq (4.0.63) we obtain

$$ln(\frac{T}{T_W}) = -1.05W^2\frac{1}{(\pi k_BT_W)^2} \tag{4.0.66}$$

Eq (4.0.66) can be written as

$$ln(1-(1-\frac{T}{T_W})) = -(1-\frac{T}{T_W}) - 1.05W^2\frac{1}{(\pi k_B T_W)^2} \tag{4.0.67}$$

Rearranging eq (4.0.67) we obtain

$$W(T) = 3.06k_B T_W\sqrt{(1-\frac{T}{T_W})} \tag{4.0.68}$$

As given in eq (4.0.68) the charge density wave order is described as a function of temperature(T) which is decreasing as temperature is increased and becomes zero at charge density wave transition temperature T_W.

Result and Discussion

Here we considerd an appropriate model Hamiltonian for a given system $YBa_2Cu_3O_y$ and double time temperature dependent Green's function formalism, we obtained mathematical expressions for the superconducting order parameter (Δ), and charge density wave order (W) and using the results we plotted the phase diagrams as given below.

Phase diagram of Superconducting order (Δ) against temperature (T)

By employing eq(4.0.40) and the experimental value, $Tc = 67K$, for $YBa_2Cu_3O_y$ at $y = 6.67$, we plotted the superconducting order parameter (Δ) versus temperature as shown in Fig.4.1. It is observed from Fig.4.1, as the temperature increases, the superconducting order parameter decreases and vanishes at the superconducting transition temperature Tc

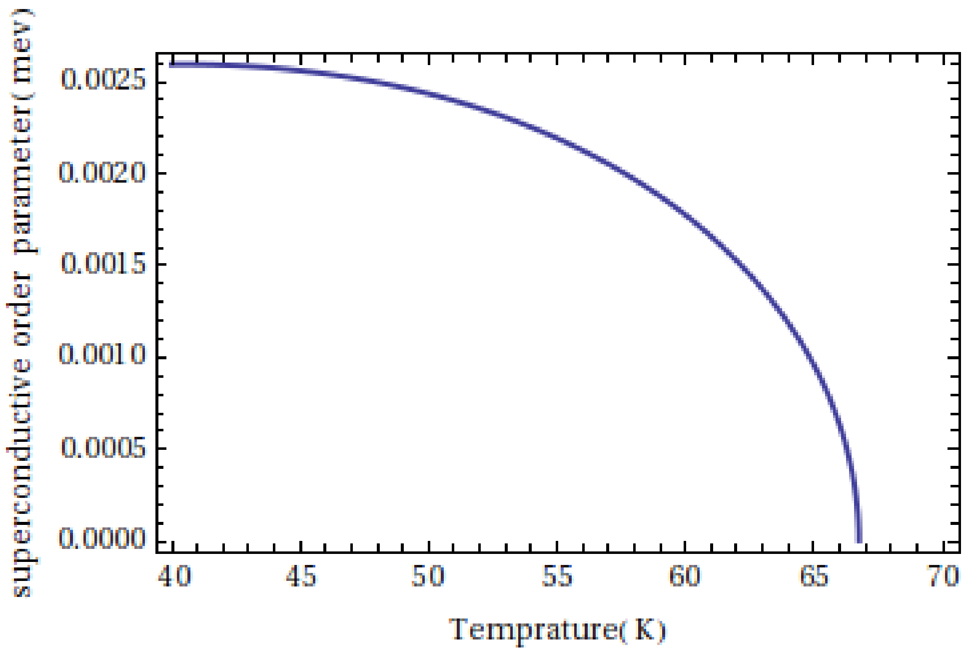

Figure 4.1: Phase diagram of Superconducting parameter (Δ) against temperature (T)

Phase Diagram Of Superconducting Order Parameter(Δ) Versus temperature(T) for different Values Of charge density wave Order parameter(W)

The expression for the superconducting order parameter as a function of temperature and charge density wave ordering has been obtained and is given in eq.(4.0.28). It is analyzed numerically for different values of the charge density wave order parameter(W). The phase diagram of the superconducting order parameter versus temperature for different values of the charge density wave ordering is plotted. As shown from Fig.4.2, the superconducting order parameter is suppressed when charge density wave ordering is set in and this suppression becomes more significant as the value of the charge density wave order parameter is larger. This suppression could be attributed to the presence of charge density wave ordering that scatters or flips the spins of the charge carriers by increasing the energy of the electrons involved in the Cooper pair and hence breaking up the pair.

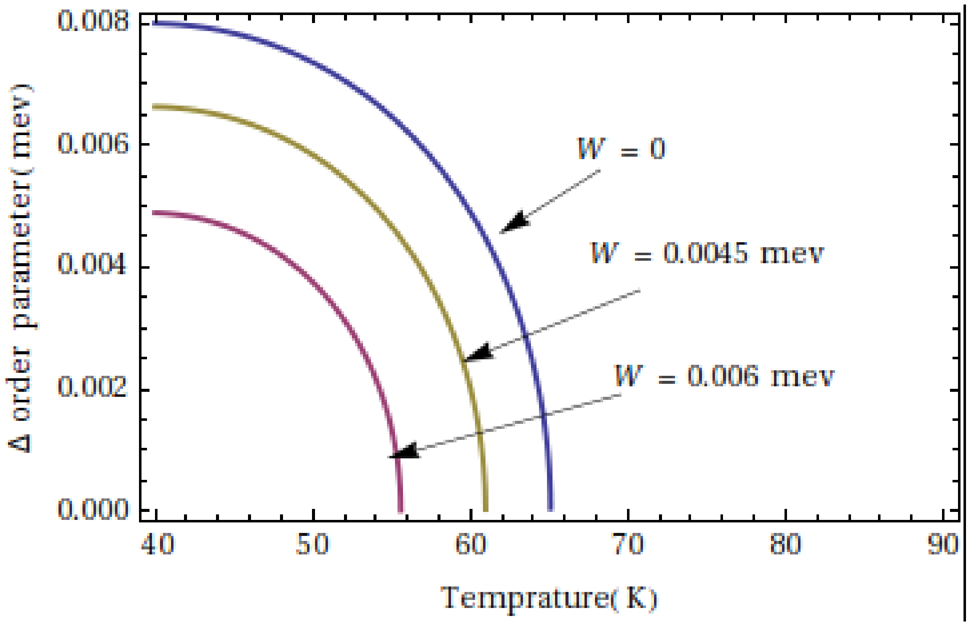

Figure 4.2: Phase diagram of Superconducting parameter(Δ) against temperature(T) for different values of charge density wave order parameter(W)

Phase diagram of charge density wave order parameter(W) against temperature (T)

By employing eq(4.0.68) and the experimental value, $T_W = 135K$, for $YBa_2Cu_3O_y$, we plotted the charge density wave order parameter(W) versus temperature as shown in Fig. 4.3. As can be observed from Fig.4.3, as the temperature increases, the charge density wave order parameter(W) decreases and vanishes at the charge density wave transition temperature T_W.

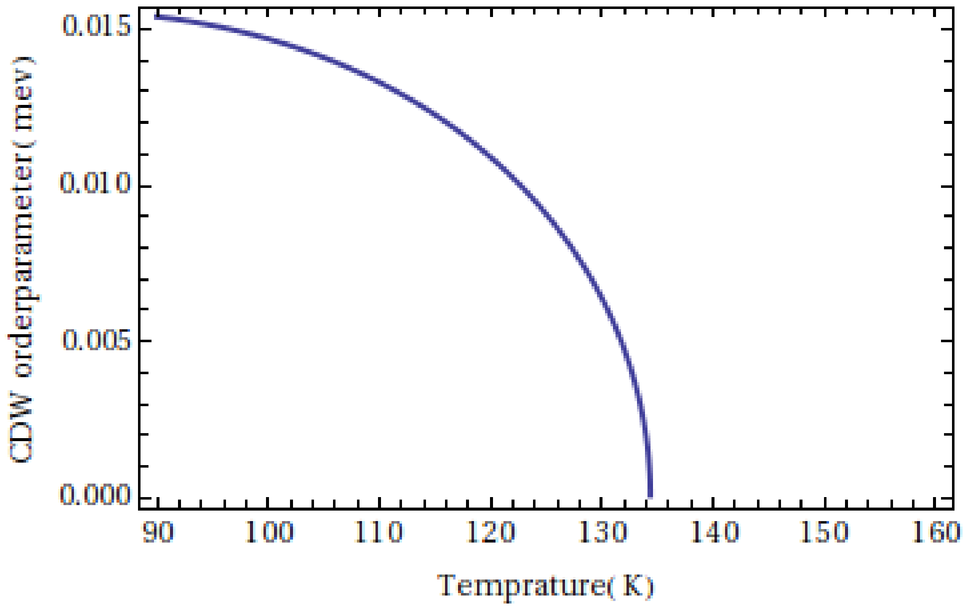

Figure 4.3: Phase diagram of charge density wave order parameter(W) against temperature (T))

Phase Diagram Of charge density wave Order parameter(W) against temperature(T) for different Values Of Superconducting Order Parameter(Δ)

By employing eq (4.0.68) and the experimental value, $T_W = 135K$, for $YBa_2Cu_3O_y$, we plotted the charge density wave order parameter(W) versus temperature (T) for different values of superconducting order parameter as shown in Fig. 4.4. As can be observed from Fig. (4.4), as the superconducting order parameter increases, the charge density wave order parameter(W) decreases. This means superconducting order parameter suppresses charge density order parameter(W).

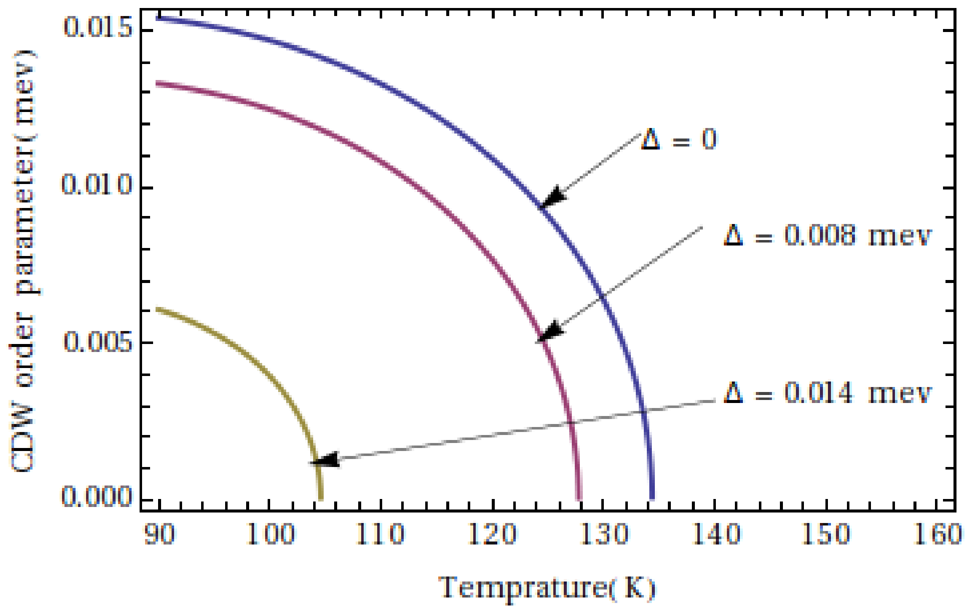

Figure 4.4: Phase diagram of charge density wave order parameter(W) against temperature (T) for different values of (Δ)

Conclusion

We have studied the interplay between charge density wave (CDW) and superconductivity in a model system by using a mean-field approximation. Following Green's functions technique and equation of motion method, we have obtained coupled equations of superconducting gap (Δ) and CDW (W) as clearly explained in eq (4.0.13) and eq (4.0.46). The two order parameters, (W) and (Δ) are coupled with each other through the distribution functions, which are also functions of (W) and (Δ). It is clear that there are three nontrivial sets of solutions for (Δ) and (W) : the pure CDW gap $\Delta = 0$, $W \neq 0$), the pure superconducting gap (W = 0, $\Delta \neq 0$), and their coexistent region ($\Delta \neq 0$ and $W \neq 0$). As clearly shown in Fig 4.2 as charge density wave increases superconductivity decreases. From fig.(4.4) as superconductivity increases charge density wave decreases. From these two figures we can say these two parameters compete each other.

Chapter 5

Competing charge, spin, and superconducting orders in underdoped $La_{2-x}Ba_xCuO_4$

Abstact

We present a model calculation of the interplay of the charge density wave (CDW), spin density wave (SDW) and superconductivity in under-doped $La_{2-x}Ba_xCuO_4$. In low doping situation the long range anti-ferromagnetic order is destroyed to give rise to SDW state accompanied by a CDW state in the system due to doping. For suitable doping the superconductivity appears in the system. The CDW state may describe the pseudogap phenomenon which co-exists with the superconducting phase and extends to normal phase in high-Tc systems. These three competing orders co-exist together. These three gap parameters are calculated from the model Hamiltonian and solved self-consistently. The theoretical results show the interplay between charge density wave, spin density wave and superconductivity in compound $La_{2-x}Ba_xCuO_4$.

Introduction

Under-doped cuprate superconductors exhibit a pseudo-gap phase that becomes apparent below a temperature T^* , where T^* decreases with increased doping, approaching the superconducting transition temperature Tc for hole concentrations beyond optimal (where optimal doping corresponds to maximum T_c)[66] . It has become common to discuss competing orders that may be responsible for the pseudo-gap and which may compete with superconductivity. There are certainly many good examples of systems where the transition temperature for one type of order, such as charge density wave (CDW) or spin density wave (SDW) order, drops to zero at the same point where the superconducting Tc reaches its maximum. From studies of $La_{2-x}Ba_xCuO_4$ it was observed that, SDW and CDW orders appear to be intertwined with a spatially modulated superconductivity [68, 69, 70]. Anti-ferromagnetic and pairing correlations seem to develop in a cooperative fashion, forming a spatially self-organized pattern. Such behavior has motivated the perspective that intertwined orders are a common feature of the cuprate superconductors [71].

The case of $La_{2-x}Ba_xCuO_4$ provides an example of how spins and charges can organize themselves in an intertwined fashion that enables strong pairing of holes. After the initial discovery of high-temperature super-conductivity[72], exploration of the phase diagram revealed a sharp minimum of T_c at the hole concentration $x \approx 1/8$. It was demonstrated that the unusual behavior in $La_{2-x}Ba_xCuO_4$ is associated with a phase transition to the low-temperature tetragonal (LTT) phase at a temperature of $\sim 60K$[74]. The occurrence of stripe order was eventually confirmed in $La_{2-x}Ba_xCuO_4$ [75, 67].

Theoretical model Hamiltonian

The purpose of this work is to study theoretically how charge density wave, spin density wave and superconductivity in $La_{2-x}Ba_xCuO_4$ superconductor compete each other. We propose the mean-field model Hamiltonian by

$$\hat{H} = \sum_{k\sigma} \epsilon_k c^\dagger_{k\sigma} c_{k\sigma} - \Delta \sum_{k\sigma} (c^\dagger_{k\uparrow} c^\dagger_{-k\downarrow} + h.c) - W \sum_{k\sigma} (c^\dagger_{k\sigma} c_{k+Q\sigma} + h.c) - M \sum_{k\sigma} (c^\dagger_{k\sigma} c_{k+Q\sigma} + h.c) \quad (5.0.1)$$

The first term in eq (5.0.1) describes the energy of free electron. Here $c^\dagger_{k\sigma}/c_{k\sigma}$ are the creation (annihilation) operators of the conduction electrons of copper atoms. The second, third and fourth terms in $\hat{H}$ describe the mean-field SC, CDW, and SDW states. The Δ , W and M are, respectively, the SC, CDW, and SDW order parameters and are given by

$$\Delta = V(0)\sum_k \langle\langle c_{k\uparrow}c_{-k\downarrow}\rangle\rangle$$

$$W = \frac{U}{2}\sum_k \langle\langle c^\dagger_{k\sigma}c_{k+Q\sigma}\rangle\rangle$$

$$M = \frac{V}{2}\sum_k \langle\langle c^\dagger_{k\sigma}c_{k+Q\sigma}\rangle\rangle$$

In order to derive an expression for superconducting order parameter we write equation of motion $\langle\langle c_{k\uparrow}, c^\dagger_{k'\uparrow}\rangle\rangle$.

$$\omega\langle\langle c_{k\uparrow}, c^\dagger_{k'\uparrow}\rangle\rangle = \delta_{kk'} + \langle\langle [c_{k\uparrow}, \hat{H}], c^\dagger_{k'\uparrow}\rangle\rangle \tag{5.0.2}$$

Putting eq (5.0,1) in eq (5.0.2)and applying anticomutation relation we get equation

$$(\omega - \epsilon_k)\langle\langle c_{k\uparrow}c^\dagger_{k\uparrow}\rangle\rangle = 1 - (M+W)\langle\langle c_{k+Q\uparrow}, c^\dagger_{k\uparrow}\rangle\rangle - \triangle\langle\langle c^\dagger_{-k\downarrow}c^\dagger_{k\uparrow}\rangle\rangle \tag{5.0.3}$$

The equation of motion for $\langle\langle c_{k+Q\uparrow}, c^\dagger_{k\uparrow}\rangle\rangle$ is

$$\omega\langle\langle c_{k+Q\uparrow}, c^\dagger_{k\uparrow}\rangle\rangle = \langle\langle [c_{k+Q\uparrow}, \hat{H}], c^\dagger_{k\uparrow}\rangle\rangle \tag{5.0.4}$$

and it gives

$$(\omega - \epsilon_{k+Q})\langle\langle c_{k+Q\uparrow}, c^\dagger_{k\uparrow}\rangle\rangle = -(M+W)\langle\langle c_{k\uparrow}, c^\dagger_{k\uparrow}\rangle\rangle \tag{5.0.5}$$

Similarly the equation of motion for $\langle\langle c^\dagger_{-k\downarrow}c^\dagger_{k\uparrow}\rangle\rangle$ can be written as

$$\omega\langle\langle c^\dagger_{-k\downarrow}, c^\dagger_{k\uparrow}\rangle\rangle = \langle\langle [c_{-k}, \hat{H}], c^\dagger_{k\uparrow}\rangle\rangle \tag{5.0.6}$$

which gives

$$(\omega + \epsilon_{-k})\langle\langle c^\dagger_{-k\downarrow}c^\dagger_{k\uparrow}\rangle\rangle = -\Delta\langle\langle c_{k\uparrow}, c^\dagger_{k\uparrow}\rangle\rangle \tag{5.0.7}$$

Substituting eq (5.0.7) in eq (5.0.3) and we obtain

$$(\omega^2 - \epsilon_k^2 - \Delta^2)\langle\langle c^{\dagger}_{-k\downarrow}, c^{\dagger}_{k\uparrow}\rangle\rangle = -\Delta + \Delta(M+W)\langle\langle c_{k+Q\uparrow}, c^{\dagger}_{k\uparrow}\rangle\rangle \tag{5.0.8}$$

Putting eq (5.0.7) in eq (5.0.5) we get

$$(\omega^2 - \epsilon_k^2 - W^2)\langle\langle c_{k+Q\uparrow}, c^{\dagger}_{k\uparrow}\rangle\rangle = -W + \Delta(M+W)\langle\langle c^{\dagger}_{-k\downarrow}, c^{\dagger}_{k\uparrow}\rangle\rangle \tag{5.0.9}$$

Solving eq (5.0.8) and eq (5.0.9) simultaneously we obtain

$$\langle\langle c^{\dagger}_{-k\downarrow} c^{\dagger}_{k\uparrow}\rangle\rangle = \frac{-\Delta}{(\omega^2 - \epsilon_k^2 - \Delta^2 - (M+W)^2))} \tag{5.0.10}$$

To take into account the temperature dependence of order parameters, we shall rewrite eq (5.0.10) as:

$$\Delta = \frac{V}{\beta}\sum_k \frac{-\Delta}{(\omega^2 - \epsilon_k^2 - \Delta^2 - (M+W)^2))}. \tag{5.0.11}$$

We replace the summation in (5.0.11) by integration. Thus

$$\sum_k = \int_{-\epsilon_f}^{\infty} N(0)d\epsilon, \tag{5.0.12}$$

where $N(0)$is the density of states at the Fermi level. Substituting eq (5.0.12) in eq(5.0.11) , we obtain,

$$\Delta = \frac{V}{\beta}N(0)\int_{-\epsilon_f}^{\infty} \frac{-\Delta}{(\omega^2 - \epsilon_k^2 - \Delta^2 - (M+W)^2))}d\epsilon. \tag{5.0.13}$$

For further simplification, we use the Matsubara frequency

$$\omega \to i\omega_n. \tag{5.0.14}$$

where , $\omega_n = \frac{(2n+1)\pi}{\beta}$. Assuming effective pairing interactions,$-\hbar\omega_b < \epsilon < +\hbar\omega_b$ and using eq (5.0.14) in eq (5.0.13)

$$1 = 2N(0)V\beta\sum_n \int_0^{\hbar\omega} \frac{d\epsilon}{(2n+1)^2\pi^2 + \beta^2 E^2}, \tag{5.0.15}$$

where $E^2 = \epsilon_k^2 + \Delta^2 + (M+W)^2$. Finally, using the Poisson summation

$$\frac{1}{2x} tanh(x/2) = \sum_n \frac{1}{(2n+1)^2\pi^2 + x^2}. \tag{5.0.16}$$

where $x = \beta E$ and defining $\lambda = VN(0)$ is the superconducting coupling constant, we can write eq(5.0.15) as

$$\frac{1}{\lambda} = \int_0^{\hbar\omega} \frac{1}{\sqrt{(\epsilon^2 + \Delta^2 + (M+W)^2)}} tanh(\beta\sqrt{(\epsilon^2 + \Delta^2 + (M+W)^2)}/2) d\epsilon \tag{5.0.17}$$

From (5.0.17), it clearly follows that the order parameters $\Delta, M\ and\ W$ for superconductivity , charge density wave and spin density wave are interdependent. Right hand side of eq (5.0.17) can be written as

$$\int_0^{\hbar\omega} \frac{tanh(\beta\sqrt{(\epsilon_k^2 + \Delta^2 + (M+W)^2)}/2 d\epsilon}{\sqrt{(\epsilon^2 + \Delta^2 + (M+W)^2)}} = \int_0^{\hbar\omega} \frac{2}{\beta} \sum_{n=-\infty}^{n=\infty} \frac{1}{\omega_n^2 + \epsilon_k^2 + \Delta^2 + (M+W)^2} \tag{5.0.18}$$

$$\int_0^{\hbar\omega} \frac{2}{\beta} \sum_{n=-\infty}^{n=\infty} \frac{1}{\omega_n^2 + \epsilon_k^2 + \Delta^2 + (M+W)^2} = \int_0^{\hbar\omega} \frac{2}{\beta} d\epsilon \sum_{n=-\infty}^{n=\infty} \frac{1}{(\omega_n^2 + \epsilon^2)} -$$

$$\int_0^{\hbar\omega} (\Delta^2 + (W+M)^2) d\epsilon \frac{2}{\beta} \sum_{n=-\infty}^{n=\infty} \frac{1}{(\omega_n^2 + \epsilon^2)^2} + .. \tag{5.0.19}$$

Using Laplaces transform and Matsubara frequency ,$\omega_n = \frac{(2n+1)\pi}{\beta}$ eq (5.0.19) can be written as

$$\frac{1}{\lambda} = \int_0^{\hbar\omega} \frac{tanh\beta\epsilon/2d\epsilon}{\epsilon} - (M+W)^2 + \Delta^2) \int_0^{\hbar\omega} d\epsilon \frac{2}{\beta} \sum_{n=-\infty}^{n=\infty} \frac{1}{((2n+1)\frac{\pi}{\beta})^2 + \epsilon^2)^2}. \tag{5.0.20}$$

It is known that

$$\sum_{n=-\infty}^{n=+\infty} \frac{1}{(((2n+1)\frac{\pi}{\beta})^2 + \epsilon^2)^2} = 2 \sum_{n=0}^{n=+\infty} \frac{1}{(((2n+1)\frac{\pi}{\beta})^2 + \epsilon^2)^2}$$

By using the relation

$$2\sum_{n=0}^{n=+\infty}\frac{1}{(a^2+\epsilon^2)^2}=2\sum_{n=0}^{n=\infty}\frac{1}{a^4(1+\frac{\epsilon^2}{a^2})^2}=2\sum_{n=0}^{n=\infty}\frac{1}{a^4(1+x^2)^2}$$

where $x=\frac{\epsilon}{a}$, and $a=\frac{1}{(2n+1)\frac{\pi}{\beta}}$. Now the right hand side of eq(5.0.20)can be written as

$$\int_0^{\hbar\omega}\frac{tanh\beta\epsilon/2d\epsilon}{\epsilon}-(M+W)^2+\Delta^2)\int_0^{\hbar\omega}d\epsilon\frac{4}{\beta}\sum_{n=0}^{n=\infty}\frac{1}{a^4(1+x^2)^2}+...=p+q. \tag{5.0.21}$$

Where

$$p=\int_0^{\hbar\omega}\frac{tanh\beta\epsilon/2d\epsilon}{\epsilon},q=(\Delta^2+(M+W)^2)\int_0^{\hbar\omega}d\epsilon\frac{4}{\beta}\sum_{n=0}^{n=\infty}\frac{1}{a^4(1+x^2)^2}+...$$

Inorder to solve for p, let $y=\frac{\beta}{2}\epsilon$. Then

$$p=\int_0^{\beta\hbar\omega/2}\frac{tanhy}{y}dy=lnytanhy-\int_0^{\beta\hbar\omega/2}lnysech^2ydy \tag{5.0.22}$$

For $\frac{\hbar\omega}{2k_BT_c}>>1, tanh\frac{\hbar\omega}{2k_BT_c}\rightarrow 1$. Extending the upper linit of the above equation we obtain

$$\int_0^{\infty}lnysech^2dy=ln\frac{\pi}{4\gamma,}$$

where $\gamma=exp(0.577)$. Simplifying eq (5.0.22) gives ,

$$p=ln\frac{\hbar\omega}{2k_BT}-ln\frac{\pi}{4\gamma}=ln1.14\frac{\hbar\omega}{k_BT} \tag{5.0.23}$$

Similarly we can solve for q as follows

$$q=(\Delta^2+(M+W)^2)\int_o^{\hbar\omega}d\epsilon\frac{4}{\beta}\sum_{n=0}^{n=\infty}\frac{1}{a^4(1+x^2)^2}=4(\Delta^2+W^2)\sum_0^{\infty}(\frac{\beta}{\pi(2n+1))})_2\int_0^{\infty}\frac{1}{(1+x^2)^2}dx+.. \tag{5.0.24}$$

$$=(\Delta^2+(M+W)^2)\frac{1}{(k_BT)^2}\frac{11}{100}$$

From standard integral we used $\int_0^{\infty}\frac{dx}{(1+x^2)^2}=\frac{\pi}{4}$ and $\sum_0^{\infty}\frac{1}{(2n+1)^2}=(1-2^{-r})\zeta(r)$ where

$r = 3, \zeta(r) = 1.202$ it is called the Riemann Zeta function. By substituting eq (5.0.24) and eq (5.0.0.23) in eq (5.0.20)we obtain

$$\frac{1}{\lambda} = ln(1.14\frac{\hbar\omega}{K_B T}) - 1.05(\Delta^2 + (M+W)^2)\frac{1}{(\pi k_B T)^2}. \tag{5.0.25}$$

From eq (5.0.25)the superconducting order parameter can be expressed interms of density waves parameters as

$$\Delta = \sqrt{[ln(1.14\frac{\hbar\omega}{k_B T}) - \frac{1}{\lambda}]\frac{(\pi k_B T)^2}{1.05} - (M+W)^2} \tag{5.0.26}$$

If charge density wave order parameter is switched off (W=0), eq (5.0.26) becomes

$$\Delta = \sqrt{[ln(1.14\frac{\hbar\omega}{k_B T}) - \frac{1}{\lambda}]\frac{(\pi k_B T)^2}{1.05} - M^2} \tag{5.0.27}$$

As can be observed from eq (5.0.26) and eq (5.0.27) as spin density order parameter(M) and sum of spin and charge density wave orders supreses superconducting order parameter shown in phase diagram Fig. 5.2. In pure superconducting phase where $W = 0, M = 0$, at Tc it can be shown that

$$\Delta(T) = 3.06 K_B T_c (1 - \frac{T}{T_c})^{1/2} \tag{5.0.28}$$

Now lets consider eq(5.0.17) in the case as

$$T \to 0, \beta \to \infty$$

then from we have

$$\frac{1}{\lambda} = \int_0^{\hbar\omega} \frac{d\epsilon}{\sqrt{(\epsilon_k^2 + \Delta^2 + (M+W)^2)}}$$

Simplifying the above expression we obtain

$$\sqrt{(\Delta^2 + (M+W)^2)} = 2\hbar\omega \exp(-\frac{1}{\lambda}) \tag{5.0.29}$$

This equation tells us that superconductivity and charge density wave can coexist in some region.

From eq(5.0.29) superconductive order (Δ) as $T \longrightarrow 0$ can be expressed as

$$\Delta(0) = \sqrt{[2\hbar\omega \exp(\frac{-1}{\lambda})]^2 - (M+W)^2)} \tag{5.0.30}$$

In the absence of density waves ordering the above equation reduces to

$$\Delta(0) = 2\hbar\omega \exp(-\frac{1}{\lambda})$$

From the BCS theory we have,

$$\frac{2\Delta(0)}{k_B T_c} = 3.5.$$

From which we get

$$k_B T_c = 1.14\hbar\omega \exp(-\frac{1}{\lambda})$$

which is the well known BCS expression for the superconducting transition temperature-Tc

5.0.3 The Spin Density Wave(SDW) Parameter(M)

In this section we derive an expression the spin density wave order parameter. To do so we calculate the equation of motion for

$$\langle\langle c^{\dagger}_{k\sigma} c_{k+Q\sigma} \rangle\rangle$$

Here we defined (σ $=\uparrow$). Using value $\hat{H}$ defined in eq (5.0.1), the equation of motion for $\langle\langle c^{\dagger}_{k\uparrow} c_{k+Q\uparrow} \rangle\rangle$ is

$$\langle\langle c^{\dagger}_{k\uparrow} c_{k+Q\uparrow} \rangle\rangle = \langle\langle [c^{\dagger}_{k\uparrow}, \hat{H}], c_{k+Q\uparrow} \rangle\rangle \tag{5.0.31}$$

Simplifying eq (5.0.31) we get

$$(\omega + \epsilon_k)\langle\langle c^{\dagger}_{k\uparrow}, c_{k+Q\uparrow} \rangle\rangle = (M+W)\langle\langle c^{\dagger}_{k+Q\uparrow} c_{k+Q\uparrow} \rangle\rangle + \Delta\langle\langle c_{-k\downarrow} c_{k+Q\uparrow} \rangle\rangle \tag{5.0.32}$$

The equation of motion for $\langle\langle c^{\dagger}_{k+Q\uparrow}, c_{k+Q\uparrow} \rangle\rangle$ is

$$\langle\langle c^{\dagger}_{k+Q\uparrow}, c_{k+Q\uparrow} \rangle\rangle = 1 + \langle\langle [c^{\dagger}_{k+Q\uparrow}, \hat{H}], c_{k+Q\uparrow} \rangle\rangle \tag{5.0.33}$$

Simplifying this we get

$$(\omega + \epsilon_{k+Q\uparrow})\langle\langle c^{\dagger}_{k+Q\uparrow}, c_{k+Q\uparrow}\rangle\rangle = 1 + (M + W)\langle\langle c^{\dagger}_{k\uparrow} c_{k+Q\uparrow}\rangle\rangle \tag{5.0.34}$$

Similarly the equation of motion for $\langle\langle c_{-k\downarrow}, c_{k+Q\uparrow}\rangle\rangle$ is

$$\langle\langle c_{-k\downarrow}, c_{k+Q\uparrow}\rangle\rangle = \langle\langle [c_{-k\downarrow}, \hat{H}], c_{k+Q\uparrow}\rangle\rangle \tag{5.0.35}$$

Simplifying this equation we get

$$(\omega - \epsilon_{-k})\langle\langle c_{-k\downarrow} c_{k+Q\uparrow}\rangle\rangle = \Delta\langle\langle c^{\dagger}_{k\uparrow}, c_{k+Q\uparrow}\rangle\rangle \tag{5.0.36}$$

Substituting eq (5.0.36) in eq (5.0.32) we get

$$(\omega^2 - \epsilon_k^2 - \Delta^2)\langle\langle c^{\dagger}_{k\uparrow} c_{k+Q\uparrow}\rangle\rangle = (\omega - \epsilon_k)(M + W)\langle\langle c^{\dagger}_{k+Q\uparrow} c_{k+Q\uparrow}\rangle\rangle \tag{5.0.37}$$

Finally solving eqs. (5.0.34) and (5.0.37)simultaneousy and solving for $\langle\langle c^{\dagger}_{k\uparrow} c_{k+Q\uparrow}\rangle\rangle$ we get

$$\langle\langle c^{\dagger}_{k\uparrow} c_{k+Q\uparrow}\rangle\rangle = \frac{(M + W)}{(\omega^2 - \epsilon_k^2 - \Delta^2 - (M + W)^2)} \tag{5.0.38}$$

The spin density wave order parameter can be expressed as:

$$M = \frac{U}{2}\sum_k \langle\langle c^{\dagger}_{k\uparrow} c_{k+Q\uparrow}\rangle\rangle \tag{5.0.39}$$

Temprature dependent of spin density wave order can be written as

$$M = \frac{U}{2\beta}\sum_k \frac{(M + W)}{\sqrt{(\omega^2 - \epsilon_k^2 - \Delta^2 - (M + W)^2)}} \tag{5.0.40}$$

The sum may be changed into an integral by introducing the density of states, N(0) and we obtain:

$$M = \frac{UN(0)}{2\beta}\int_0^{\hbar\omega} \frac{(M + W)d\epsilon}{\sqrt{(\omega^2 - \epsilon_k^2 - \Delta^2 - (M + W)^2)}} \tag{5.0.41}$$

For further simplification, we use the Matsubara frequency

$$\omega \rightarrow i\omega_n,$$

where

$$\omega_n = \frac{(2n+1)\pi}{\beta}$$

Considering the fact that effective pairing interactions is found in region $-\hbar\omega < \epsilon < \hbar\omega$, eq (5.0.41) becomes

$$-M = 2VN(0)\beta \sum_{0} \int_{0}^{\hbar\omega} \frac{(M+W)d\epsilon}{(2n+1)^2\pi^2 + \beta^2 E^2} \tag{5.0.42}$$

where $E^2 = \epsilon_k^2 + \Delta^2 + (M+W)^2$. Finally, using the Poisson summation

$$\frac{1}{2x} tanh(\frac{x}{2}) = \sum_{n} \frac{1}{(2n+2)^2\pi^2 + x^2} \tag{5.0.43}$$

where $x = \beta E$ and defining $\eta = VN(0)$ is spin density wave coupling constant, eq(5.0.41) becomes

$$\frac{-M}{\eta} = \int_{0}^{\hbar\omega} \frac{(M+W)}{\sqrt{(\epsilon_k^2 + \Delta^2 + (M+W)^2)}} tanh(\beta\sqrt{(\epsilon_k^2 + \Delta^2 + (M+W)^2}/2)d\epsilon \tag{5.0.44}$$

From eq(5.0.44), it is again indicates that the order parameters Δ, M and W are interdependent. Therefore, we can assume that in some temperature interval, charge density wave, spin density wave and superconductivity may co-exist and compete each other.

Competing superconducting (Δ) and spin density wave(M) orders in under-doped $La_{2-x}Ba_xCuO_4$

In this section we study the effect of spin density wave order(M) on superconducting order parameter (Δ). Now let consider eq (5.0.44) by switching off charge density wave order(W=0) which is given by

$$\frac{-1}{\eta} = \int_{0}^{\hbar\omega} \frac{1}{\sqrt{(\epsilon_k^2 + \Delta^2 + M^2)}} tanh(\beta\sqrt{(\epsilon_k^2 + \Delta^2 + M^2)}/2)d\epsilon \tag{5.0.45}$$

Right hand side of eq (5.0.45) can be written as

$$\int_0^{\hbar\omega} \frac{tanh(\beta\sqrt{(\epsilon_k^2+\Delta^2+M^2)}/2d\epsilon}{\sqrt{(\epsilon^2+\Delta^2+M^2)}} = \int_0^{\hbar\omega} \frac{2}{\beta}\sum_{n=-\infty}^{n=\infty}\frac{1}{\omega_n^2+\epsilon_k^2+\Delta^2+M^2} \tag{5.0.46}$$

$$\int_0^{\hbar\omega} \frac{2}{\beta}\sum_{n=-\infty}^{n=\infty}\frac{1}{\omega_n^2+\epsilon_k^2+\Delta^2+M^2} = \int_0^{\hbar\omega}\frac{2}{\beta}d\epsilon\sum_{n=-\infty}^{n=\infty}\frac{1}{(\omega_n^2+\epsilon^2)} - \int_0^{\hbar\omega}(M^2+\Delta^2)d\epsilon\frac{2}{\beta}\sum_{n=-\infty}^{n=\infty}\frac{1}{(\omega_n^2+\epsilon^2)^2}+.... \tag{5.0.47}$$

Using Laplaces transform and Matsubara frequency ,$\omega_n = \frac{(2n+1)\pi}{\beta}$ eq (5.0.47) can be written as

$$\frac{-1}{\eta} = \int_0^{\hbar\omega}\frac{tanh\beta\epsilon/2d\epsilon}{\epsilon} - (M^2+\Delta^2)\int_0^{\hbar\omega} d\epsilon\frac{2}{\beta}\sum_{n=-\infty}^{n=\infty}\frac{1}{((2n+1)\frac{\pi}{\beta})^2+\epsilon^2)^2}. \tag{5.0.48}$$

It is known that

$$\sum_{n=-\infty}^{n=+\infty}\frac{1}{(((2n+1)\frac{\pi}{\beta})^2+\epsilon^2)^2} = 2\sum_{n=0}^{n=+\infty}\frac{1}{(((2n+1)\frac{\pi}{\beta})^2+\epsilon^2)^2}$$

By using the relation

$$2\sum_{n=0}^{n=+\infty}\frac{1}{(a^2+\epsilon^2)^2} = 2\sum_{n=0}^{n=\infty}\frac{1}{a^4(1+\frac{\epsilon^2}{a^2})^2} = 2\sum_{n=0}^{n=\infty}\frac{1}{a^4(1+x^2)^2}$$

where $x = \frac{\epsilon}{a}$, and $a = \frac{1}{(2n+1)\frac{\pi}{\beta}}$. Now the right hand side of eq (5.0.48)can be written as

$$\int_0^{\hbar\omega}\frac{tanh\beta\epsilon/2d\epsilon}{\epsilon} - (M^2+\Delta^2)\int_0^{\hbar\omega} d\epsilon\frac{4}{\beta}\sum_{n=0}^{n=\infty}\frac{1}{a^4(1+x^2)^2} + ... = p+q. \tag{5.0.49}$$

Where

$$p = \int_0^{\hbar\omega}\frac{tanh\beta\epsilon/2d\epsilon}{\epsilon}, q = (\Delta^2+M^2)\int_0^{\hbar\omega} d\epsilon\frac{4}{\beta}\sum_{n=0}^{n=\infty}\frac{1}{a^4(1+x^2)^2} + ...$$

Inorder to solve for p, let $y = \frac{\beta}{2}\epsilon$. Then

$$p = \int_0^{\beta\hbar\omega/2}\frac{tanhy}{y}dy = lnytanhy - \int_0^{\beta\hbar\omega/2} lnysech^2ydy \tag{5.0.50}$$

For $\frac{\hbar\omega}{2k_BT_c} >> 1, tanh\frac{\hbar\omega}{2k_BT_c} \to 1$ Extending the upper limit of the above equation we obtain

$$\int_0^\infty lny sech^2 dy = ln\frac{\pi}{4\gamma,}$$

where $\gamma = exp(0.577)$. Simplifying eq (5.0.50) gives

$$p = ln\frac{\hbar\omega}{2k_BT} - ln\frac{\pi}{4\gamma} = ln1.14\frac{\hbar\omega}{k_BT} \tag{5.0.51}$$

Similarly we can solve for q as follows

$$q = (\Delta^2 + M^2)\int_o^{\hbar\omega} d\epsilon\frac{4}{\beta}\sum_{n=0}^{n=\infty}\frac{1}{a^4(1+x^2)^2} = 4(\Delta^2 + M^2)\sum_0^\infty(\frac{\beta}{\pi(2n+1))})_2\int_0^\infty\frac{1}{(1+x^2)^2}dx + .. \tag{5.0.52}$$

$$= (\Delta^2 + W^2)\frac{1}{(k_BT)^2}\frac{11}{100}$$

From standard integral we used $\int_0^\infty \frac{dx}{(1+x^2)^2} = \frac{\pi}{4}$ and $\sum_0^\infty \frac{1}{(2n+1)^2} = (1-2^{-r})\zeta(r)$ where $r = 3, \zeta(r) = 1.202$ it is called the Riemann Zeta function. By substituting eq (5.0.51) and eq (5.0.52) in eq (5.0.48)we obtain

$$\frac{-1}{\eta} = ln(1.14\frac{\hbar\omega}{K_BT}) - 1.05(\Delta^2 + M^2)\frac{1}{(\pi k_BT)^2}. \tag{5.0.53}$$

From eq(5.0.53)the spin density wave order parameter can be expressed in terms of superconducting order parameter as

$$M = \sqrt{[ln(1.14\frac{\hbar\omega}{k_BT}) + \frac{1}{\eta}]\frac{(\pi k_BT)^2}{1.05} - \Delta^2} \tag{5.0.54}$$

As can be observed from eq (5.0.54) as superconducting ordeder increases spin density order parameter is getting supressed as clearly shown in phase diagram Fig (5.3).

Competing charge density wave(W) and spin density wave(M) orders in under-doped $La_{2-x}Ba_xCuO_4$

In this section we study how charge density wave(W) and spin density wave(M) orders compete each other in under-doped $La_{2-x}Ba_xCuO_4$. To do so lets consider eq (5.0.44) by switching off superconducting order parameter ($\triangle = 0$) which is given by

$$\frac{-M}{\eta} = \int_0^{\hbar\omega} \frac{(M+W)}{\sqrt{(\epsilon_k^2 + (M+W)^2)}} tanh(\beta\sqrt{(\epsilon_k^2 + (M+W)^2}/2) d\epsilon \tag{5.0.55}$$

From eq (5.0.55) we get

$$\frac{-M}{\eta(M+W)} = \int_0^{\hbar\omega} \frac{1}{\sqrt{(\epsilon_k^2 + (M+W)^2)}} tanh(\beta\sqrt{(\epsilon_k^2 + (M+W)^2}/2) d\epsilon \tag{5.0.56}$$

We calculated eq (5.0.56) applying the same technique we used above which is expressed as

$$\frac{-M}{\eta(M+W)} = ln 1.14 \frac{\hbar\omega}{k_B T} - 1.05 [\frac{(M+W)}{\pi k_B T}]^2 \tag{5.0.57}$$

From eq (5.0.57) we have

$$(M+W) = \sqrt{[ln(1.14 \frac{\hbar\omega}{k_B T}) + \frac{M}{\eta(M+W)}] \frac{(\pi k_B T)^2}{1.05}} \tag{5.0.58}$$

From eq(5.0.58) we have the expression for spin density wave order as a function of temprature(T) and charge density wave order as

$$M = \sqrt{[ln(1.14 \frac{\hbar\omega}{k_B T}) + \frac{M}{\eta(M+W)}] \frac{(\pi k_B T)^2}{1.05}} - W \tag{5.0.59}$$

From eq (5.0.59) in pure spin density wave order at spin density wave transition temperature $T = T_M$ we have

$$\frac{-1}{\eta} = ln 1.14 \frac{\hbar\omega}{k_B T_M} \tag{5.0.60}$$

In pure spin density wave region from eq(5.0.55) we have

$$\frac{-1}{\eta} = \int_0^{\hbar\omega} \frac{1}{\sqrt{(\epsilon_k^2 + M^2}} tanh(\beta\sqrt{(\epsilon_k^2 + M^2}/2) d\epsilon \tag{5.0.61}$$

simplifying this eq (5.0.55)as usual we obtain

$$\frac{-1}{\eta} = ln 1.14\frac{\hbar\omega}{k_B T} - 1.05 M^2 \frac{1}{(\pi k_B T_M)^2} \tag{5.0.62}$$

Comparing eq (5.0.60) and eq (5.0.62) we obtain

$$ln(1.14\frac{\hbar\omega}{k_B T_M}) = ln 1.14\frac{\hbar\omega}{k_B T} - 1.05 M^2 \frac{1}{(\pi k_B T_M)^2} \tag{5.0.63}$$

from which we obtain

$$M(T) = 3.06 k_B T_M \sqrt{(1 - \frac{T}{T_M})} \tag{5.0.64}$$

Result and Discussion

In this chapter , we considered the interplay of three strongly competing orders, namely superconductivity, charge density wave and spin density wave in the under-doped $La_{2-x}Ba_xCuO_4$. The single particle electron Greens functions are calculated using Zubarevs technique from which the gap equations for superconducting order parameter (Δ) , charge density wave order parameter (W) ,spin density wave order parameter (M), superconducting transition temperature Tc charge density wave transition temperature (T_W)spin density wave transition temperature (T_M). Based on these expressions,by taking into account the experimental values needed parameters we plotted and discussed the phase diagrams for various combinations of these parameters.

The phase diagram of superconducting order against temperature for under-doped $La_{2-x}Ba_xCuO_4$

By employing eq(5.0.28) and the experimental value, $T_c = 16K$, for $La_{2-x}Ba_xCuO_4$, we plotted the superconducting order parameter (Δ) versus temperature as shown in Fig.5.1. As can be observed from Fig. 5.1, as the temperature increases, the superconducting order parameter decreases and vanishes at the superconducting transition temperature Tc

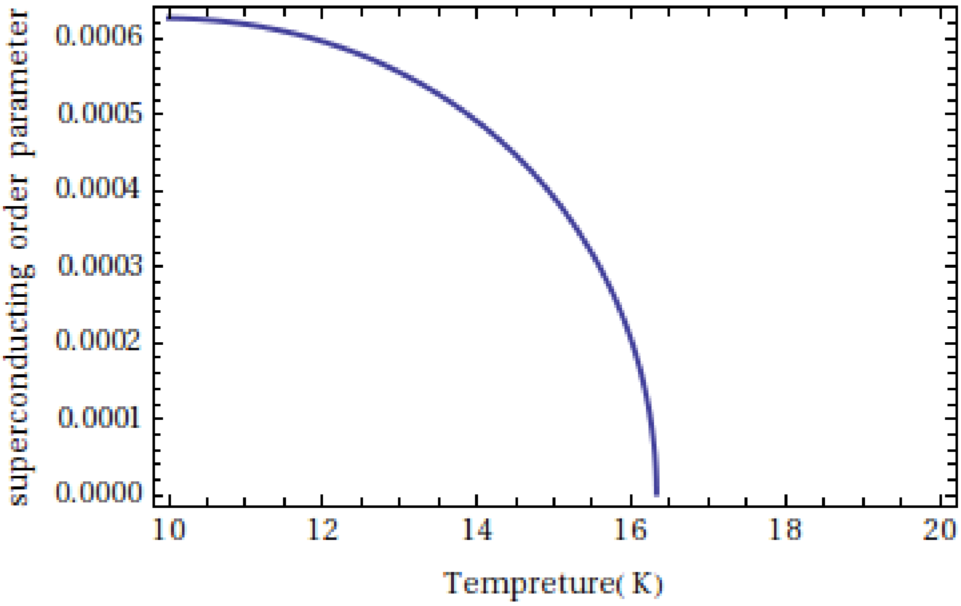

Figure 5.1: Phase diagram of Superconducting parameter (Δ) against temperature (T)

Phase Diagram Of Superconducting Order Parameter(Δ) Versus temperature(T) for different Values Of charge density wave Order parameter(W)and spin density wave order parameter (M)

The expression for the superconducting order parameter as a function of temperature and charge density wave ordering(W) and spin density wave ordering (M) has been obtained and is given in eq.(5.0.26). It is analyzed numerically for different values of the charge density wave order parameter(W) and spin density wave orders. The phase diagram of the superconducting order parameter versus temperature for of different values of the charge density wave ordering and spin density wave ordering is plotted. As shown from Fig.5.2, the superconducting order parameter is suppressed when charge density wave ordering and spin density wave ordering are increased and this suppression becomes more significant as the value of the charge and spin density wave order parameter increases. This suppression could be attributed to the presence of charge and spin density wave ordering that scatters or flips the spins of the charge carriers by increasing the energy of the electrons involved in the Cooper pair and hence breaking up the pair.

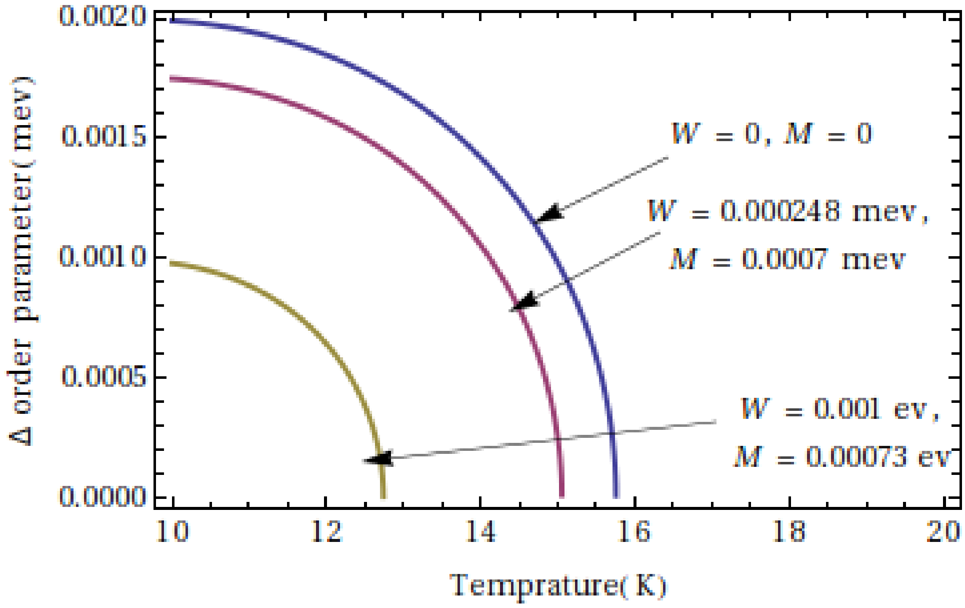

Figure 5.2: Phase diagram of Superconducting parameter (Δ) against temperature(T) for different values of charge density wave order parameter(W) and spin Density wave order (M)

The phase diagram of spin density wave order against temperature for under-doped $La_{2-x}Ba_xCuO_4$

By employing eq (5.0.64) and the experimental value, $T_M = 42K$, for $La_{2-x}Ba_xCuO_4$, we plotted the spin density wave order parameter (M) versus temperature as shown in Fig.5.3. As can be seen from Fig. 5.3, as the temperature increases, the SPIN density wave order parameter decreases and vanishes at the spin density wave transition temperature T_M.

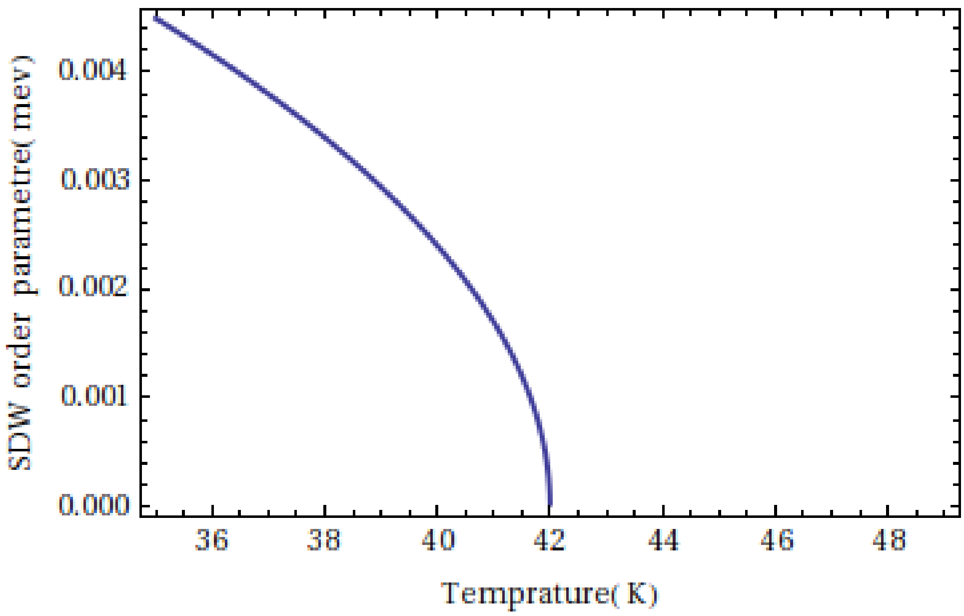

Figure 5.3: Phase diagram of spin density wave order (M) against temperature (T)

The phase diagram of spin density Density wave order against temperature for underdopped $La_{2-x}Ba_xCuO_4$ for different values of superconducting order parameter(Δ

) By employing eq (5.0.54) and the experimental value, $T_M = 42K$, for $La_{2-x}Ba_xCuO_4$, we plotted the spin density wave order parameter (M) versus temperature for different values of superconducting order parameters as shown in Fig. 5.4, as superconducting order parameter increases, the spin density wave order parameter decreases.

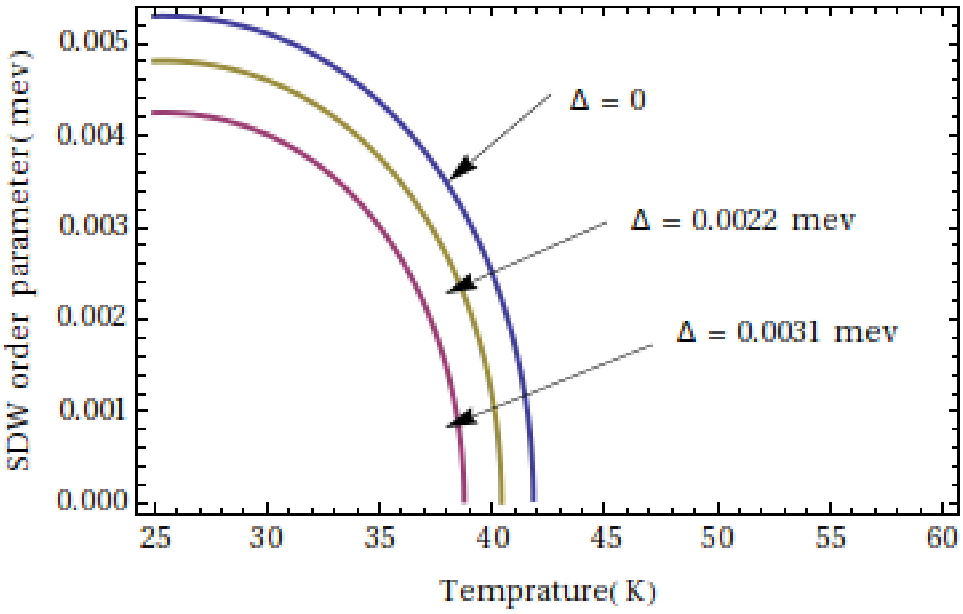

Figure 5.4: Phase diagram of spin density wave order (M) against temperature (T) for different values of (Δ)

.

Chapter 6

Combined Mechanisms in high temperature Superconductors

Abstact

While phonons are central to explaining the mechanism of conventional superconductivity, their role should be taken into account for explaining copper-based superconductivity, as well. It is suggested that phonons have a role in the superconductivity mechanism in Fe- pnictides also. We studied the dependence of the superconductive transition critical temperature Tc for some systems, where superconductivity is mediated by a combined phonon- exciton mechanism for cuprate and a combined phonon-magnon mechanism for pnictides. It is believed that purely electronic mechanisms of high-temperature superconductivity are not sufficient alone and unable to capture the essential physics of cuprates and other layered superconductors, but the combination with phonon does[106, 113, 115, 116].

Introduction

The isotope effect has played an important role in the understanding of the underlying pairing mechanism in superconductors. Historically it was used to identify the role of the electron-lattice interaction for the superconductivity. Experimental evidence as to the nature of interaction that causes superconductivity were first provided in 1950 by Maxwell [108] and by Reynolds et al. [109] . They showed that $T_c \propto M^{-\alpha}$, where $\alpha = 0.5$ and M is the mean mass of different isotopes of the superconductor. These findings indicated that the ion mass, and therefore lattice vibrations, phonons, are important to the mechanism of superconductivity.

Frohlich [110], who was unaware of the experiments on the isotope effect, and Bardeen [111], the same year, have provided theories of the phonon-electron interaction, which in turn led to models of superconductivity dependent on the phonon energies.

For the high-Tc superconductors the study of the isotope effect does not paint a simple and straightforward picture. The role of the electron-lattice interactions in the mechanism of superconductivity was initially ruled out, and the pairing mechanism was ascribed to antiferromagnetic exchange and fluctuations [78, 79]. As time went it was observed that interactions of the lattice with the carriers in high-T_c became important [80, 81, 82, 83].

Excitonic superconductivity was first suggested as a theoretical possibility in 1964 by Little [84] and Ginzburg [85, 86]. The idea is very similar to that involving phonons, except that the polarization leading to an attractive interaction is not due to a movement of the ions themselves but rather to movements of electrons (say, on the ion cores perhaps not within the superconducting CuO planes). This polarization will result in a net positively charged region of space to which a conduction electron will be attracted. Little envisioned a one-dimensional geometry with conduction chains along side "exciton" chains. The two types of electrons (conduction and those that produce the excitons) are then physically separated from one another. Ginzburg considered a two-dimensional geometry with a metallic layer sandwiched between two dielectric layers.

The most compelling reason for considering excitonic superconductivity is, in that the mediating boson (exciton) now has an electronic energy scale. Hence, in the simple BCS picture, Tc; will be significantly enhanced because the prefactor is now $\omega_{ex} >> \omega_D$. Theoretical work [103] has also suggested the possiblity of excitonic superconductivity in the high-Tc oxides[107].

Phonon -exciton combined mechanism in cuprates

The understanding of the mechanism responsible for the high superconducting transition temperature of the cuprate superconductors has remained elusive in spite of the enormous effort devoted to its study during the past thirty years.

There is as yet no consensus as to the mechanism that is responsible for the superconductivity of the high-Tc oxides[103] . One possibility that is being explored is that it is a combined phonon-plus-excitonic mechanism[104, 105, 113, 114]

W. A. Little et al using Resonant Inelastic X-Ray Scattering (RIXS) now provide compelling evidence of the nature of the interactions that cause the high transition temperature of the optimally doped cuprates. The high transition temperatures suggested that excitations with energies above those of the phonons would be involved[113, 114, 115]. If this were so, tunneling would be unable to yield the density of states at these energies, because the voltages required would exceed the breakdown potential of the barrier [116]. However, it has long been known that similar information from that of tunneling can be obtained from the optical properties[117, 118] of a superconductor. They observed that a phonon-electron interaction was needed as well as interactions at energies between 1.6 and 2.3 eV. From their experimental observations they make the following conclusions.

i) Little et al [113, 114, 115] found that electron-phonon interaction alone, while moderately strong, is much too weak to explain the high transition temperature of the materials.

ii) There are no contributions to the pairing in the mid-infrared region between 0.1 and 1.0eV that might be expected from some magnetic or plasmon interactions.

iii)The key feature in explaining the high transition temperature is the combination of a phonon interaction and the high energy electronic contributions [119]. Neither one alone, results in a high transition temperature nor is able to account for the optical properties.Both are needed.

iv) There is a clear indication of an attractive contribution from higher energy interactions that exceeds the repulsive Coulomb interaction at these energies[120].

v)The real and imaginary parts of the gap function give a characteristic shape to the energy dependence of the calculated reflectance ratio. This is accurately mapped in the observed reflectance ratio both in the phonon and in the electronic-interaction regions. This fingerprint is strong evidence that the Eliashberg equations accurately describe the superconducting gap function even at energies that are many times higher than the phonon energies for which the theory was developed.At high energies the integral could be approximated to:

$$Re[\frac{\sigma_s(\omega}{\sigma_N(\omega)}] \approx 1 - \frac{2\Delta_0 Re[\Delta(\Delta - \Delta_0)] ln \frac{2\omega}{\Delta_o}}{\omega^2} \tag{6.0.1}$$

Equation (6.0.1) shows a reduction occurs in the above ratio where the gap function (Δ) becomes large, as in the neighborhood of the electronic terms between 1 and 2 eV for many of the cuprates. Their data shows such depletion. Molegraaf et al.also observed such depletion in the oscillator strength sum rule [121]for $Bi_2Sr_2CaCu_2O_{8+\delta}$ using spectroscopic ellipsometry.

One of the main attractions of the proposed phonon- exciton combined mechanism by Singh and Sinha [91] is the apparent possibility of higher transition temperatures which follows from modified BCS formula for Tc is given by

$$T_c = 1.14\omega_{ph}^{h1}\omega_e^{h2}\exp[-(\lambda_{ph}^* + \lambda_e^*)^{-1}] \tag{6.0.2}$$

where λ_e is the electron(hole) exciton coupling constant and ,ω_{ph} and ω_e are energies of phononic and elecronic excitations respectively. $h_1 = \frac{\lambda_{ph}}{(\lambda_{ph}+\lambda_e)}$, $h_2 = \frac{\lambda_e}{(\lambda_{ph}+\lambda_e)}$, $\lambda_{ph}^* = \frac{\lambda_{ph}}{(\lambda_{ph}+1)}$, $\lambda_e^* = \frac{\lambda_e}{(\lambda_e+1)}$ In this section we calculate T_c values for some cuprates using eq(6.0.2) by using $\omega_{ph} = 300k$, $\lambda_{ph} = 0.33$, $\omega_e = 4000K$ and different values of λ_e and compare with experimentally observed values as reported in the table below.

Table 6.1: Comparison between theoretical and experimental value of superconducting transition temperatures for cuprates.

Compounds	λ_e	Experimental value of Tc(K)	Theoretical value of Tc(K)
$YBa_2Cu_3O_7$	0.218	92	92.42
$Bi_2Sr_2CaCu_2O_8$	0.20	85	84.62
$Bi_2Sr_2Ca_2Cu_3O_{10}$	0.245	110	109.8
$TlBa_2Ca_3Cu_4O_{11}$	0.264	122	122.15
$HgBa_2Ca_2Cu_3O_8$	0.28	134	134.11

Phonon -magnon mechanism of Pairing in pnictides

Despite extensive studies on high-Tc superconductivity in iron pnictides since its discovery, the question of what plays an important role in the pairing mechanism of this class of superconductors remains enigmatic. The earlier estimated value of the electron-phonon coupling within the

Eliashberg theory was found to be very weak to generate the required Tc for these systems,[93, 94] and as a result an unconventional origin of superconductivity mediated by AFM spin-fluctuations was proposed[95]. In another study, the effect of magnetization and doping was calculated on the electron-phonon coupling, and it was found that electron-phonon coupling strength increases significantly via spin-channels [96, 97]. Theoretical calculations have also suggested that electronic structure of FeBS systems is strongly perturbed below the magnetic transition temperature due to the opening of spin density wave gap[98, 99]. The electron-phonon coupling increases substantially for states at the Fermi surface due to anisotropic coupling between phonons and magnetic moments (i.e. magneto-elastic coupling) in the AFM structure below structural and magnetic transition temperature. The strength of the electron-phonon coupling constant, calculated by taking into account the many body effects is found to be ($\lambda_{e-p} \sim 1$), suggesting that the role of electron-phonon coupling can not be neglected in the pairing mechanism. In addition to these theoretical calculations, a large isotope coefficient as high as $\alpha_{fe} \sim 0.81$ has been reported experimentally for different families of FeBS,[100, 101, 102] clearly suggesting that the electron-phonon coupling can not be ruled out in understanding the pairing mechanism in these materials along with other degrees of freedom such as spin and orbital.

Existing reports in the literature, with finite iron isotope coefficient in different families of FeBS, suggest that the study of isotope effect is pertinent to investigate the role of electron-phonon coupling in these materials.

The magnetic mechanism of pairing in high-temperature superconductors was studied by many researchers. These studies used the assumption that the pairing is realized due the exchange by spin excitations magnons, i.e., the transfer system is the system of spins in a magnetic metal.

A great attention was attracted by the pioneer work by Akhiezer and Pomeranchuk[89, 90]. They considered the interaction between conduction electrons caused by both the exchange by acoustic phonons and an additional interaction related to the exchange by spin waves (magnons).

Egami et al [91] had also suggested that spin-phonon coupling may play an important role in the superconductivity of iron pnictides.

In this section, by taking into consideration the combined role of phonon-plus-magnon mechanism of pairing following Singh and Sinha [91] we calculated Tc values for some iron based compounds using

$$T_c = 1.14\omega_{ph}^{h1}\omega_{sf}^{h2}\exp[-(\lambda_{ph}^* + \lambda_{sf}^*)^{-1}] \tag{6.0.3}$$

where λ_{sf} is the spin fluctuation electron coupling constant and, ω_{ph} and ω_{sf} are energies of phononic and spin fluctuation excitations respectively, $h_1 = \frac{\lambda_{ph}}{(\lambda_{sf}+\lambda_{ph})}$, $h_2 = \frac{\lambda_{sf}}{(\lambda_{ph}+\lambda_{sf})}$, $\lambda_{ph}^* = \frac{\lambda_{ph}}{(\lambda_{ph}+1)}$, $\lambda_{sf}^* = \frac{\lambda_{sf}}{(\lambda_{sf}+1)}$ and compare the results with experimentally observed values. Using $\omega_{ph} = 300k$, $\lambda_{ph} = 0.33$, $\omega_{sf} = 1000K$ and different values of λ_{sf} we get Tc values for various iron based compounds as reported in the table below.

Table 6.2: Comparison between theoretical and experimental value of super- conducting transition temperatures for iron pnictides.

Compounds	λ_{sf}	Experimental value of Tc(K)	Theoretical value of Tc(K)
$LaO_{1-x}F_xFeAs$	0.11	26	26.32
$Ba_{1-x}K_xFe_2As2$	0.16	38	38.65
$Fe_{1-y}Se_xTe_{1-x}$	0.06	15	15.75
$SmO_{1-x}F_xFeAs$	0.23	56	56.5
$Ca_{1-x}Nd_xFeAsF$	0.232	57	57.33

We have described as comprehensively as possible our view regarding the role of exciton -plus- phonon as pairing mechanism in a number of novel superconducting systems, paying special attention to the cuprates and the role magnon -plus- phonon as pairing mechanism for pnictides. We have indicated how phonon combined with exciton/magnon as a mechanism can give rise to high temperature superconductivity, and it can be shown theoretically even room temperature is possible within this framework[91].

Chapter 7

SUMMARY AND CONCLUSION

By using a model Hamiltonian consisting of charge density wave and superconducting part and applying Green's function formalism we derived an expression for charge density wave order parameter and superconducting order parameters for $YBaCuOy$ system. We have presented the theoretical curve of the superconducting order parameter $\Delta(T)$ for different values of charge density wave(CDW) order parameter. It is observed that as charge density wave(CDW) order parameter increases the superconducting order parameter decreases. Again we plotted the graph of charge density wave order parameter against temperature for different values of superconducting order parameter. It is observed that as superconducting order parameter increases charge density wave(CDW) order parameter decreases. Then we can say that superconducting and charge density wave orders compete in certain temperature interval. Similarly by using a model Hamiltonian consisting of charge density wave, spin density wave, and superconducting order parameter parts and applying Green's function formalism we derived an expressions for for each of these parameters for $La_{2-x}Ba_xCuO_4$ system. From these expressions we can easily observe that these three order parameter compete each other in certain temperature interval. Finally we discussed combined phonon-exciton and phonon-magnon as mechanisms for cuprates and pnictides high-Tc superconductor respectively. We calculated the theoretical high-Tc values for some cuprates and pinicides giving appropriate values for the desired parameters and we got values approximately comparable to their corresponding experimentally determined results.

Bibliography

[1] Andrei Marouchkine, *Room-Temperature Superconductivity*, Cambridge International Science Publishing, First published (2004)

[2] H. Kamerlingh. Onnes, Akad. *V. Wetenschappel* **14**, 113(1911)

[3] W. Meissner and R. Ochsenfeld. *Naturwiss* **21**. 787(1933)

[4] F. London and H. London. *Proc. Roy. Soc. (London)* **A149**:71(1935).

[5] V. L. Ginzburg and L. D. Landau.*Zh. Eksp. Teor. Fiz.* **20**1064(1950).

[6] J. Bardeen, L. N. Cooper, and J. R. Schrieffer.*Phys. Rev.* **108**, 1175(1957).

[7] W. L. McMillan.*Phys. Rev.* **167**, 331(1968).

[8] B. T. Matthias et al., *Phys. Rev. A,* **139**:1501 (1965).

[9] J. G. Bednorz and K. A. M uller. Z.*Phys. B: Condens. Matter* **64**, 189(1986).

[10] M. K. Wu et al, *Phys. Rev. Lett.* **58**, 908(1987).

[11] A. Schilling et al, *Nature* **363**, 56(1993).

[12] R. J. Cava et al, *Nature* **367**, 146(1994).

[13] J. Nagamatsu et al., *Nature (London)* **410**, 63(2001)

[14] Y. Kamihara et al., *J. Am. Chem. Soc.* **130**, 3296(2008).

[15] C. Wang et el, *Lett.* **83**, 134(2008)

[16] F. London and H. London, *Proa R. Soc. (Lond.)***A149**, 71(1935).

[17] E. Maxwell, *Phys. Rev.* **78**, 477(1950)

[18] C. A. Reynolds et al.,*Phys. Rev.* **78**, 467(1950)

[19] H. Frolich, *Phys. Rev.* **79**, 845(1950)

[20] D. N. Zubarev, *Sov. Phys. USPE* **3**, 320(1960)

[21] Drozdov A. P et al., arXiv:1412.0460 (1 December 2014).

[22] Drozdov A. P et al.,*Nature* **525**, 73(2015)

[23] Ge et al *Phys. Rev. B* **93**, 4513(2016)

[24] C. S. Gorter and H. Casimir. Zeitschrift fr*Technische Physik* 15:539 .

[25] F. London and H. London.*Proc. Roy. Soc. (London)* **A149**, 71(1935).

[26] A. P. Mackenzie and Y. Maeno. *Rev. Mod. Phys.* **75**, 657(2003).

[27] C. C. Tsuei and J. R. Kirtley.*Rev. Mod. Phys.* **72**, 969(2000).

[28] J. Bardeen et al, *Phys. Rev* **106 (1)**, 162(1957).

[29] J. Bardeen et al, *Phys. Rev.* **108 (5)**, 1175(1957).

[30] L. Gao et al, *Phys. Rev. B* **50**, 4260(1994)

[31] N. E. Bickers et al., *Int. J. Mod. Phys. B* **1**, 687(1987)

[32] S. Doniach, *Physica B.* **91**, 231(1977).

[33] Shoji TANAKA *Japanese Journal of Applied Physics* **45**, 12(2006).

[34] Presland et al,*Physica C* **176**, 95(1991)

[35] Obertelli et al, *Phys. Rev. B* **46**, 14928(1992).

[36] Sun et al. *Physics Letters A* **192(1)**, 122(1994)

[37] Andrea Damascelli and Zhi-Xun Shen. *Reviews of Modern Physics* **75(2)**, 473(2003).

[38] M. Imada et al, *Reviews of Modern Physics* **70(4)**, 1039(1998).

[39] Jaejun Yu et al. *Physical Review Letters* **58(10)**, 1035(1987).

[40] Y. Kamihara et al. *Journal of the American Chemical Society* **130**, 3296(2008)

[41] Z.A. Ren et al, *Europhysics Letters* **82**, 57002(2008).

[42] H. Kito et al,*Journal of the Physical Society of Japan* **77**, 063707(2008).

[43] M. Rotter et al, *Physical Review Letters* **101**, 107006(2008).

[44] J. Zhao,et al, *Nature Materials* **7**, 953(2008).

[45] S. A. J. Kimber et al, *Nature Materials* **8**, 471(2009).

[46] M. Wang et al., *Physical Review B* **81**, 174524(2010).

[47] McMahon et al, *Rev. Mod. Phys.* **84**, 1607(2012).

[48] Nagamatsu et al., *Nature* **410**, 63(2001).

[49] J.G.Bednorz and K.A.Muller,*Z.Phys. B* **64**, 189(1989).

[50] Wu.K.M et al, *Phys.Rev.Lett.* **58**, 908(1987).

[51] Schilling A et al., *Nature* **363**, 56(1993)

[52] Gao.L.etal, *Phys.* **50**, 4260(1994).

[53] C.Wang et al, *Europhys.Lett.* **83**, 67006(2008).

[54] R. E. Peierls, *Quantum Theory of Solids* (Clarendon, New York,(2001).

[55] G. Gruner, *Rev. Mod. Phys.* **60**, 1129(1988).

[56] P. A. Lee et al, *Phys. Rev. Lett.* **31**, 462(1973).

[57] Ghiringhelli, G. et al.,*Science* **337**, 821(2012)

[58] Achkar et al., *Phys. Rev. Lett.* **109**, 167001(2012).

[59] Chang et al, . *Nat. Phys.* **8**, 871(2012). .

[60] da Silva Neto et al ., *Science* **347**, 282(2015).

[61] Wu et al.*Nature* **477**, 191(2011).

[62] Cyr-Choinie et al. Preprint at http://arxiv.org/abs/1503.02033 (2015).

[63] Comin, R. *Nat. Mater.* **14**, 796(2015).

[64] Achkar et al, Preprint at http://arxiv.org/abs/ 1409.6787(2014).

[65] Sachdev, S. and La Placa, R. .*Phys. Rev Lett.* **111**, 027202(2013).

[66] M. R. Norman et al,*Physica C* **162**, 1491(1989c).

[67] M. Hcker et al, *Phys. Rev. B* **83** , 104506 (2011)

[68] A. Himeda et al, it Phys. Rev. Lett. **88**, 117001(2002).

[69] E. Berg et al,*Phys. Rev. Lett.* **99**, 127003(2007).

[70] E. Berg et al,*New J.Phys.* **11**, 115004(2009).

[71] E. Fradkin et al., arXiv:1407.4480(2014)

[72] J. Bednorz, K. Muller, Z.*Phys. B* **64** , 189193 (1986).

[73] T. Nagano et al,*Phys. Rev. B*, **48** 9689-9696 (1993).

[74] J. D. Axe at el, *Phys. Rev. Lett.*, **62**, 2751 (1989)

[75] M. Fujita et al, *Phys. Rev. B* **70**, 104517 (2004)

[76] P. Singh, et al, *J. Solid State Commun.* **73**, 45(1990)

[77] J. Chang et al, *Nat.Phys.* **8**, 871(2012).

[78] .P. W. Anderson, *Science* **235**, 1196(1987).

[79] D. J. Scalapino, *Phys. Rep.* **250**, 329(1995).

[80] G.-H. Gweon et al, *Nature* **430**, 187(2004).

[81] A. Bussmann-Holder et al, *Europhys. Lett.* **72**, 423(2005)

[82] J. Hwang et al, *Nature* **E3**, 446(2007).

[83] A. R. Bishop et al, *J. Supercond.Nov. Magn.* **20**, 393(2007).

[84] W. A. Little, *Phys. Rev.* **134**, 1416(1964)

[85] 'V. L. Ginzburg et al, *Fiz. Nauk* **101**, 185(1970)

[86] V. L Ginzburg and D. A. Kirzhnits,*in Soviet-American Symposium on Electron Theory of Solids*, Leningrad, (1971)

[87] G. Y. Wang et al,*Phys. Rev. B* **75**, 212503(2007).

[88] Wolf , *Novel Superconductivity* (1987)

[89] A. I. Akhiezer and I. Ya. Pomeranchuk, *Zh. Eksp. Teor. Fiz.* **36**, 819(1959).

[90] A. I. Akhiezer et al, *North-Holland, Amsterdam* , **369**(1968).

[91] Singh, P and Sinha, K.P.J. *Sol. Sta. Commun.* **73**, 45(1990).

[92] Egami T et al, arXiv:0908.4361(2009)

[93] L. Boeri et al, *Phys. Rev. Lett.* **101**, 026403(2008).

[94] T. Yildirim, *Phys. Rev. Lett.* **102**, 037003(2009).

[95] I. I. Mazin et al.,*Phys. Rev. Lett.* **101**, 057003(2008).

[96] L. Boeri et al., arXiv: 0902.0288.

[97] T. Egami et al., arXiv: 0908.4361.

[98] F. Yndurain and J. M. Soler,*Phys. Rev. B* **79**, 134506(2009).

[99] M. L. Kulic and A. A. Haghighirad,*Europhys. Lett.* **87**, 17007(2009).

[100] R. H. Liu et al., *Nature* **459**, 64(2009).

[101] P.M. Shirage et al., *Phys. Rev. Lett.* **103**, 257003(2009).

[102] P.M. Shirage et al.,*Phys. Rev. Lett.* **105**, 037004(2010).

[103] Wolf et al, *Novel Superconductivity (Plenum, New York)* (1987).

[104] Marsiglio et al, *Solid State Commun.* **64**, 905(1987b)

[105] Marsiglio et al, *Physica C* **227**, 153(1988)

[106] Marsiglio, F., and J. P. Carbotte, *Phys. Rev. B* **36**, 3937(1987b).

[107] Yu et al, *Phys. Lett. A* **122**, 203(1987).

[108] E. Maxwell,*Phys. Rev.* **78** , 477 (1950).

[109] C. A. Reynolds et al, *Phys. Rev.* **78**, 487(1950).

[110] H. Frohlich,*Phys. Rev.* **79** , 845 (1950)

[111] J. Bardeen,*Phys. Rev.*, **79** , 167 (1950).

[112] Anderson, P. W., *Science* **235** , 1196 (1987)

[113] W. A. Little, *Phys. Rev.* **134**, 1416(1964).

[114] V. L. Ginzburg, Sov.*Phys. JETP* **47**, 2318(1964).

[115] W.A.Little in Novel Superconductivity, eds.,Wolf, S. A., and Kresin, V. Z (Plenum, (New York) 341, (1987)

[116] W.A.Little and J. P.Collman, Proc. *Nat. Acad. Sci USA* **85**, 4596(1988).

[117] S.B.Nam,*Phys. Rev.* **156**, 470(1967).

[118] W.Shaw and J.C. Swihart,*Phys. Rev. Lett.* **20**, 1000(1968).

[119] M.J.Holcomb, *Phys. Rev. B* **54**, 6648(1996)

[120] M.J.Holcomb et. *Phys. Rev. B* **53**, 6734(1996).

[121] H.J.A.Molegraaf et al., *Science* **295**, 2239(2002).

[122] Md. Atikur Rahman et al, *American Journal of Physics and Applications* ;**3(2)**: 39-56(2015)

[123] Mun K.Chan,et al,*Proceedings of the National Academy of Sciences*, **110(30)**:1223512240, (2013)

[124] F.C. Hsu et.al *Proc. Natl.Acad. Sci. U.S.A.* **105**, 14262(2008).

[125] Robert E. Thorne, Charge Density Wave Conductors, *Phys. Today* **49(5)**, 42 (1996)

Publication

1.Urga Dinegde, P Singh: Competing Superconductivity (Δ) and Charge-density Wave(W) in $YBa_2Cu_3O_y$ [under review].

2.Urga Dinegde, P Singh: Competing superconductivity(Δ), CDW(W) and SDW (M)in $La_{2-x}Ba_xCuO_4$ [under review].

DECLARATION

I hereby declare that this PhD dissertation is my original work, has not been presented for a degree in any other University and that all the sources of material used for the dissertation have been dully acknowledged.

Name: Urga Dinegde

Signature: ____________________

This PhD dissertation has been submitted for examination with my approval as University advisor.

Name: prof. P. Singh

Signature: ____________________

Place and time of submission:

Addis Ababa University,

March 2018